Crystal-Structure-Based Design and Synthesis of Benz[*cd*]indole-Containing Inhibitors of Thymidylate Synthase[1]

Michael D. Varney,* Gifford P. Marzoni, Cindy L. Palmer, Judith G. Deal, Stephanie Webber, Katherine M. Welsh, Russell J. Bacquet, Charlotte A. Bartlett, Catharine A. Morse, Carol L. J. Booth, Steven M. Herrmann, Eleanor F. Howland, Robert W. Ward, and Jennifer White

Agouron Pharmaceuticals, Inc., 3565 General Atomics Court, San Diego, California 92121. *Received July 30, 1991*

The X-ray crystal-structure-based design, synthesis, and biological activity of a novel family of benz[*cd*]indole-containing inhibitors of thymidylate synthase (TS) are described. The structure–activity of the lead compound was studied by conceptually dividing the molecule into four regions and independently optimizing the substituents for each region. Combination of favored substituents for each region led to inhibitors with K_i's against the human enzyme in the range of 10–20 nM. Thymidine shift experiments suggested that the cytotoxic properties of the best enzyme inhibitors were due to TS targeting in cells. The inhibitors were synthesized from substituted 6-aminobenz[*cd*]indol-2(1*H*)-ones by alkylation with both a simple alkyl group and a substituted benzylic portion. The 2,6-diaminobenz[*cd*]indoles were prepared from the corresponding lactams by conversion to the thiolactam, alkylation to the methylated thiolactam, and then displacement with a substituted or unsubstituted amine.

Introduction

Thymidylate synthase (TS) (EC 2.1.1.45) catalyzes the reductive methylation of deoxyuridylate (dUMP) to thymidylate (dTMP), and in addition, oxidatively demethylates its cofactor 5,10-methylenetetrahydrofolate (THF) to dihydrofolate. Outside of salvage pathways, TS is the sole source of dTMP and interruption of its function can, and usually does, result in cell death. Because of its crucial role in DNA synthesis, TS has been much studied as an anticancer target, and clinically relevant human antitumor activity has been demonstrated with compounds that bind at either the cofactor or the substrate binding sites.[2] 5-Fluorodeoxyuridine monophosphate (FdUMP, 1), the TS-active metabolite of 5-fluorouracil (5-FU) is an

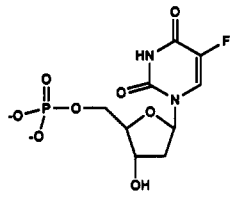

1 FdUMP

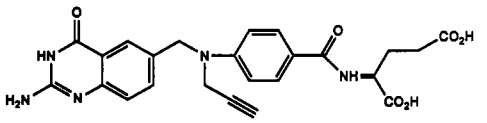

2

example of a substrate analogue, and N^{10}-propargyl-5,8-dideazafolic acid (2) is the classic example of a potent folate site inhibitor.[3] From a structural standpoint, the common link between these and essentially all other TS inhibitors is their striking similarity to the natural substrate or cofactor. Their development is a classical case of designing metabolic antagonists. In light of the fact that many enzymes and receptors bind nucleotides and folate cofactors, such an analogue design program can suffer from an inherent lack of target selectivity. For example, 5-FU in addition to acting against TS (as FdUMP) can be incorporated as a nucleoside triphosphate into RNA, resulting in some unfavorable toxicities.[4] Many glutamate-containing folate analogues are known to inhibit both DHFR and TS,[5] and as a result, interpretation of in vitro and in vivo results are sometimes difficult. Active transport of glutamate-containing antifolates into cells is a process critical to their cytotoxicity[6] which ultimately can lead to mechanisms of resistance.[7]

As a possible way to avoid many of the problems outlined above, we began a program to design lipophilic TS inhibitors for use as antitumor agents using as a primary guide the information contained in the X-ray crystal structure of *Escherichia coli* TS.[8] We chose to pursue lipophilic TS inhibitors because they should passively

(1) This paper has been presented in part at the 202nd Meeting of the American Chemical Society, Joint Meeting with the European Federation of Medicinal Chemistry, held in New York City on August 25–30, 1991.

(2) (a) Berman, E. M.; Werbel, L. M. The Renewed Potential for Folate Antagonists in Contemporary Cancer Chemotherapy. *J. Med. Chem.* **1991**, *34*, 479–485. (b) Douglas, K. T. The Thymidylate Synthesis Cycle and Anticancer Drugs. *Med. Res. Rev.* **1987**, *7*, 441–475 and references cited therein.

(3) Jones, T. R.; Calvert, A. H.; Jackman, A. L.; Brown, S. J.; Jones, M.; Harrap, K. R. A Potent Antitumor Quinazoline Inhibitor of Thymidylate Synthetase: Synthesis, Biological Properties and Therapeutic Results in Mice. *Eur. J. Cancer* **1981**, *17*, 11.

(4) (a) Myers, C. E. The Pharmacology of the Fluoropyrimidines. *Pharmacol. Rev.* **1981**, *33*, 1–15. (b) Maybaum, J.; Ullman, B.; Mandel, H. G.; Day, J. L.; Sadee, W. Regulation of RNA- and DNA-Directed Actions of 5-Fluoropyrimidines in Mouse T-Lymphoma (S-49) Cells. *Cancer Res.* **1980**, *40*, 4209–4215. (c) Wilkinson, D. S.; Tlsty, T. D.; Hanas, R. J. The Inhibition of Ribosomal RNA Synthesis and Maturation in Novikoff Hepatoma Cells by 5-Fluorouridine. *Cancer Res.* **1975**, *35*, 3014–3020.

(5) (a) Hynes, J. B.; Patil, S. A.; Tomazic, A.; Kumar, A.; Pathak, A.; Tan, X.; Xianqiang, L.; Ratnam, M.; Declamp, T. J.; Freisheim, J. H. Inhibition of Murine Thymidylate Synthase and Human Dihydrofolate Reductase by 5,8-Dideaza Analogues of Folic Acid and Aminopterin. *J. Med. Chem.* **1988**, *31*, 449–454. (b) Calvert, A. H.; Jones, T. R.; Dady, P. J.; Grzelakowska-Sztabert, B.; Paine, R. M.; Taylor, G. A.; Harrap, K. R. Quinazoline Antifolates with Dual Biochemical Loci of Action. Biochemical and Biological Studies Directed Towards Overcoming Methotrexate Resistance. *Eur. J. Cancer* **1980**, *16*, 713–722.

(6) (a) Henderson, G. B.; Strauss, B. P. Characteristics of a Novel Transport System for Folate Compounds in Wild-Type and Methotrexate-Resistant L1210 Cells. *Cancer Res.* **1990**, *50*, 1709–1714. (b) Nair, M. G.; Galivan, J.; Maley, F.; Kisliuk, R. L.; Ferone, R. Transport, Inhibition of Tumor Cell Growth and Unambigous Synthesis of 2-Desamino-2-Methyl-N^{10}-Propargyl-5,8-Dideazafolate (DMPDDF) and Related Compounds. *Proc. Am. Assoc. Cancer Res.* **1989**, *30*, 476.

(7) Fry, D. W.; Jackson, R. C. Membrane Transport Alterations as a Mechanism of Resistance to Anticancer Agents. *Cancer Surveys* **1986**, *5*, 47–79.

(8) The unavailability of the X-ray structure of the human TS necessitated the use of the *E. coli* enzyme in design. The assumption that the *E. coli* structure is an accurate representation of the human structure is based on the fact that of the 28 residues in contact with the inhibitors, only two are different. For further details see ref 10.

0022-2623/92/1835-0663$03.00/0

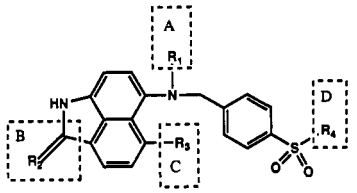

Figure 1. General structure of benz[*cd*]indole-containing inhibitors. Regions designated A–D represent areas on which structure–activity studies were performed.

diffuse in and out of cells and will therefore not be susceptible to resistance due to lack of transport.[9] As a result, lipophilic TS inhibitors should have a different spectrum of antitumor activity than the classical glutamate-containing inhibitors such as methotrexate and N^{10}-propargyl-5,8-dideazafolic acid (**2**). Such a structure-based design exercise should result in the generation of completely novel inhibitors that are uniquely designed to fit TS and therefore should be highly selective in their mechanism of cell growth inhibition.

Herein we report the successful completion of such an investigation and present the design, synthesis, and biological activity of a novel class of benz[*cd*]indole-containing TS inhibitors represented in Figure 1. These compounds bind at the folate binding site of TS, as shown by X-ray crystallography, but show very little resemblance to the natural cofactor. In addition, thymidine reversal experiments suggest that the more potent compounds in this series are cytotoxic due to TS inhibition.

Design

We have previously described our approach to crystal-structure-based inhibitor design and the de novo design and crystallographic analysis of the lead in this series of benz[*cd*]indole-containing inhibitors, compound **3**.[10] The inhibition constants against human and *E. coli* TS were determined to be 3 and 38 μM, respectively. Since this indicated that **3** was roughly 200–1000 times weaker a TS inhibitor than N^{10}-propargyl-5,8-dideazafolic acid (**2**),[3] we felt that significantly greater enzyme affinity would be required for useful antitumor activity.

It was determined crystallographically that the tricyclic portion of **3** binds in the deep hydrophobic part of the folate binding pocket of the *E. coli* TS as illustrated in Figure 2. The naphthalene ring makes hydrophobic contacts at the top and bottom of the site. The lactam NH hydrogen bonds to conserved Asp 169, but the lactam carbonyl oxygen makes unfavorable steric and electrostatic interactions with the carbonyl oxygen of Ala 263. The

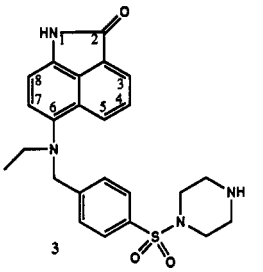

N-alkyl substituents make hydrophobic interactions with Trp 80 and Phe 176. The benzylic portion of the inhibitor bound in *E. coli* TS is shown in Figure 3. In this area, the benzene ring exits the active site through a narrow opening and the *p*-SO_2 group enables the piperazine ring to make contact with a hydrophobic wall, made up primarily of the side chain of Ile 79, on the periphery of the protein.

The crystal-structure analysis suggested four distinct regions of the molecule where structural changes were anticipated to lead to improved binding. These four areas are shown in Figure 1 and are labeled A–D. The optimization of compound **3** was viewed as a four-variable matrix problem. Treating each variable as independent, we would optimize substituents in regions A–D of the molecule individually and ultimately combine these in order to obtain the best inhibitors.

All potential inhibitors were modeled by overlaying a minimized structure of the inhibitor[11] onto the crystal structure of either lactam **3** or amidine **12** bound in *E. coli* TS.[10] Compounds were minimized from a number of different conformations in order to gain information about the conformational preferences of the molecule and to ensure that the modeled conformation was not more than 3 kcal above the minimum-energy conformation. Compounds with substituents that appeared to visually complement the protein optimally in the particular region of interest (i.e. by means of space filling, hydrogen bonding, and/or electrostatic complimentarity) were chosen for synthesis.

For synthetic reasons, the first area investigated was the N-6 alkyl substituent, region A. GRID analysis[12] indicated that substituents in this area bind in a hydrophobic pocket formed in part by Trp 80. Deeper into the pocket near Glu 58 and a number of bound water molecules, the area becomes hydrophilic. Since the GRID results are difficult to compare quantitatively from one substituent to another, this analysis could only suggest possible types of substituents for each particular part of the site. For example, the GRID maps for a methyl probe are concentrated around the pocket formed by Trp 80, and the hydroxy and other hydrophilic probes were concentrated around Glu 58 and the bound water molecules. Modeling did not reveal clear advantages for larger or smaller substituents in the hydrophobic area. However, the water molecules deep in the pocket could be targets for replacement by hydrogen-bonding substituents at the tip of an alkyl chain. Shown in Table I are the results of this structure–activity study. In all, eight derivatives were synthesized and the isopropyl,

(9) Some lipophilic quinazoline TS inhibitors have been reported: (a) McNamara, D. J.; Berman, E. M.; Fry, D. W.; Werbel, L. M. Potent Inhibition of Thymidylate Synthase by Two Series of Nonclassical Quinazolines. *J. Med. Chem.* **1990**, *33*, 2045–2051. (b) Jones, T. R.; Varney, M. D.; Webber, S. E.; Welsh, K. M.; Webber, S.; Matthews, D. A.; Appelt, K.; Smith, W. S.; Janson, C.; Bacquet, R.; Lewis, K. K.; Marzoni, G. P.; Kathardekar, V.; Howland, E.; Booth, C.; Herrmann, S.; Ward, R.; Sharp, J.; Moomaw, E.; Bartlett, C.; Morse, C. New Lipophilic Thymidylate Synthase Inhibitors Designed from the X-Ray Structure of the *E. coli* Enzyme. *Proc. Am. Assoc. Cancer Res.* **1990**, *31*, A2016.

(10) Appelt, K.; Bacquet, R. J.; Bartlett, C. A.; Booth, C. L. J.; Freer, S. T.; Fuhry, M. M.; Gehring, M. R.; Herrmann, S. M.; Howland, E. F.; Janson, C. A.; Jones, T. R.; Kan, C.; Kathardekar, V.; Lewis, K. K.; Marzoni, G. P.; Matthews, D. A.; Mohr, C.; Moomaw, E. W.; Morse, C. A.; Oatley, S. J.; Ogden, R. C.; Reddy, M. R.; Reich, S. H.; Schoettlin, W. S.; Smith, W. W.; Varney, M. D.; Villafranca, J. E.; Ward, R. W.; Webber, S.; Webber, S. E.; Welsh, K. M.; White, J. Design of Enzyme Inhibitors Using Iterative Protein Crystallographic Analysis. *J. Med. Chem.* **1991**, *34*, 1925–1934.

(11) All small molecules were minimized using the semiempirical AM1 method: Dewar, M. J. S.; Zoebisch, E. G.; Healy, E. F.; Stewart, J. J. P. AM1: A New General Quantum Mechanical Molecular Model. *J. Am. Chem. Soc.* **1985**, *107*, 3902. Modeling was conducted using Polygen Corporation's Quanta program on a Silicon Graphics 4D70GT.

(12) Goodford, P. J. A Computational Procedure for Determining Energetically Favorable Binding Sites on Biologically Important Macromolecules. *J. Med. Chem.* **1985**, *28*, 849.

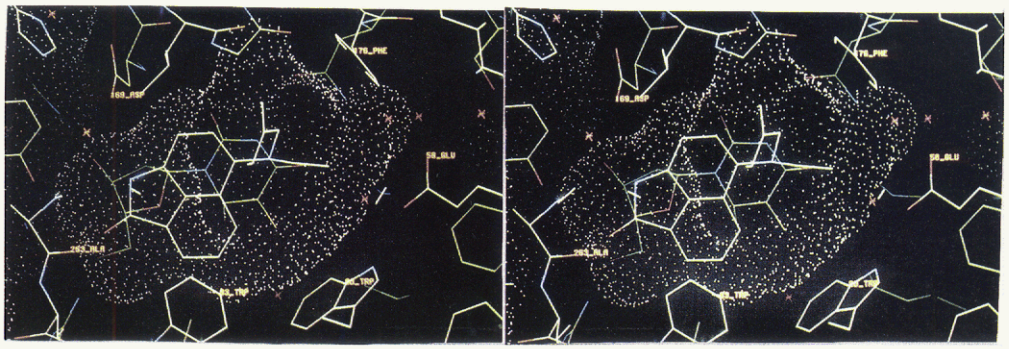

Figure 2. Stereo drawing showing the X-ray structure of compound **3** complexed with *E. coli* TS. The tricyclic portion of the inhibitor is shown and the principle points of contact with the active site residues are labeled.

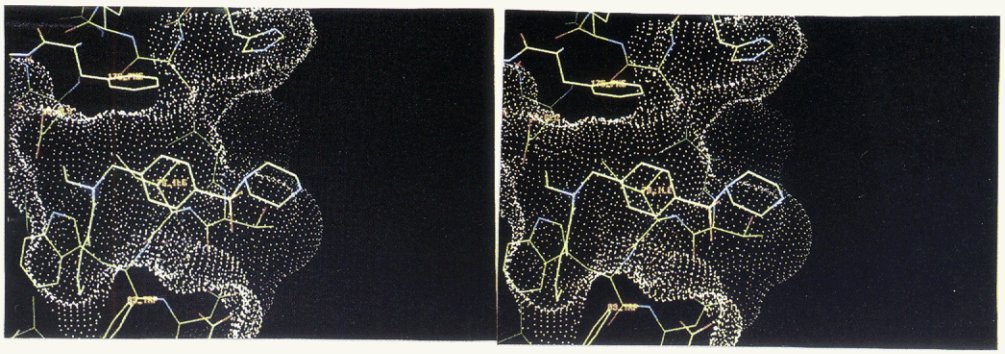

Figure 3. Stereo drawing showing the X-ray structure of compound **3** complexed with *E. coli* TS. The benzylic portion of the inhibitor is shown and the principle points of contact with the active site residues are labeled.

Table I. Effect of Changing Substituents in Region A

					E. coli K_i,[a] μM		human K_i,[a] μM		IC_{50},[b] μM		
no.	R^1	R^2	R^3	R^4	K_{is}	K_{ii}	K_{is}	K_{ii}	L1210	CCRF-CEM	GC_3/M TK$^-$
3	C_2H_5	O	H	piperazinyl	38	36	3.0	1.6	6.0	4.1	16
4	*n*-C_3H_7	O	H	piperazinyl	>30[c]	>30[c]	13	11	2.9	3.1	5.4
5	*i*-C_3H_7	O	H	piperazinyl	18	27	11	5.7	3.9	6.8	5.9
6	CH_2CH_2OH	O	H	piperazinyl	6.5	12	0.59	0.88	50	31	>50[c]
7	$CH_2CH_2CH_2OH$	O	H	piperazinyl	39	92	6.9	8.8	21.5	15.0	30.0
8	CH_2SCH_3	O	H	phenyl	>1[c]	>1[c]	5.0	2.8	2.1	2.8	>10.0[c]
9	CH_3	O	H	piperazinyl	21	29	0.84	0.52	2.3	8.3	25.0
10	H	O	H	phenyl	>3[c]	>3[c]	2.6	2.8	2.3	>4.0[c]	>4.0[c]

[a] TS activity was assayed by the tritium release method of Lomax and Greenberg[31] with some modifications. Reported K_i values have an average standard deviation of 33%. See Experimental Section for a detailed description. [b] Inhibition of cellular growth was measured with a modification[32] of the MTT[33] colorimetric assay of Mosemann.[34] See Experimental Section for a detailed description. [c] The insolubility of the inhibitory compound prevented any value from being determined.

hydroxyethyl, and methyl substituents, compound **5**, **6**, and **9**, were found to be optimal for the *E. coli* enzyme. Compounds **6** and **9** were found to be optimal for the human enzyme. These results are consistent with the GRID analysis, but in this case, GRID was not helpful in distinguishing between the hydroxyethyl (**6**) and the hydroxypropyl (**7**) whose activity differed by a factor of 6–10. We believe that the methyl group is better than other substituents because it makes a better steric interaction with the conserved tryptophan residue 80.[10] Unfortunately, we were unable to obtain a crystal structure of compound **6** in complex with TS and so can only speculate that it either displaces one or more of the water molecules, thus gaining binding free energy by primarily entropic contributions, or interacts with them in a favorable manner resulting in a net enthalpic gain. The fact that two of the compounds are optimal against both the human and *E. coli* enzymes is encouraging in that it suggests that for some substituents, the *E. coli* structure is an accurate surrogate for the human enzyme in this region.

Switching to region B, we felt that the hydrogen-bonding pattern of the lactam function was not optimal due to an unfavorable interaction with the carbonyl oxygen of Ala 263. We reasoned that either removing the lactam carbonyl or allowing some other substituent in that position to hydrogen bond with the Ala 263 carbonyl oxygen would result in improved binding. Table II shows the results of these studies. In all, five derivatives were synthesized. Compounds **11**–**15** were synthesized to investigate changes in hydrogen-bonding patterns. All of these except compound **13** resulted in improved inhibition. The optimal substituents were found to be the primary amine group as in amidine **12** and the *N*-methyl amidine **15**. The explanation for this is 2-fold. The measured pK_a of **12** is in the range of 8.2,[13] indicating that the inhibitors are probably bound in the protonated form. Such a positively charged molecule would enhance the already favorable hydrogen-bonding interaction of the NH with the Ala 263

(13) Potentiometric titrations were performed at 25 °C as described by Albert and Serjeant (Albert, A.; Serjeant, E. P. *The Determination of Ionization Constants. A Laboratory Manual*, 3rd ed.; Chapman and Hall: New York, 1984.) in *N*,*N*-dimethylformamide/H_2O (67:33).

Table II. Effect of Changing Substituents in Region B

no.	R^1	R^2	R^3	R^4	*E. coli* K_i,[a] μM		human K_i,[a] μM		IC_{50},[b] μM		
					K_{is}	K_{ii}	K_{is}	K_{ii}	L1210	CCRF-CEM	GC_3/M TK⁻
11	C_2H_5	NH	H	phenyl	7.1	22	0.4	0.081	0.7	1.25	3.0
12	CH_3	NH	H	phenyl	1.5	3.2	0.031	0.030	0.38	1.6	4.6
13	CH_3	NNH_2	H	phenyl	>10[c]	>10[c]	1.9	2.5	2.4	1.3	>10[c]
14	CH_3	NOH	H	phenyl	6.1		0.36	0.73	0.81	2.0	>5.0[c]
15	CH_3	NCH_3	H	phenyl	2.1	4.7	0.053	0.054	1.6	3.3	3.4

[a-c] See footnotes in Table I.

Table III. Effect of Changing Substituents in Region C

no.	R^1	R^2	R^3	R^4	*E. coli* K_i,[a] μM		human K_i,[a] μM		IC_{50},[b] μM		
					K_{is}	K_{ii}	K_{is}	K_{ii}	L1210	CCRF-CEM	GC_3/M TK⁻
16	CH_3	O	CH_3	phenyl	3.0	3.4	0.073	0.070	1.9	4.8	>5[c]
17	CH_3	NH	CH_3	phenyl	0.21	0.55	0.035	0.044	0.25	0.36	0.52
18	CH_3	O	Cl	morpholinyl	3.1	3.5	0.12	0.075	>5[c]	>5[c]	>5[c]
19	CH_3	NH	Cl	morpholinyl	1.6	2.1	0.029	0.020	0.44	0.9	1.4
20	CH_3	NH	SCH_3	morpholinyl	0.23	0.54	0.11	0.11	1.9	3.1	6.9

[a-c] See footnotes in Table I.

Table IV. Effect of Changing Substituents in Region D

no.	R^1	R^2	R^3	R^4	*E. coli* K_i,[a] μM		human K_i,[a] μM		IC_{50},[b] μM		
					K_{is}	K_{ii}	K_{is}	K_{ii}	L1210	CCRF-CEM	GC_3/M TK⁻
21	C_2H_5	O	H	phenyl	>1[c]	>1[c]	1.3	1.0	3.05	>3.33[c]	>3.33[c]
22	CH_3	O	H	4-hydroxyphenyl	2.9	6.0	0.20	0.06	10.0	9.5	9.5
23	CH_3	O	H	4-methoxyphenyl	>2[c]	>2[c]	0.27	0.18	4.6	3.0	>10.0[c]
24	CH_3	O	H	4-aminophenyl	4.5	7.4	0.14	0.079	9.1	5.9	>10.0[c]
25	CH_3	O	H	morpholinyl	6.6	11	0.30	0.25	>5.0[c]	>5.0[c]	>5.0[c]
26	CH_3	O	H	4-nitrophenyl	>10[c]	>10[c]	0.11	0.18	2.0	2.8	>5.0[c]
27	CH_3	NH	H	morpholinyl	1.8	5.4	0.012	0.015	0.49	0.46	0.9
28	CH_3	NH	H	4-methoxyphenyl	1.4	2.5	0.025	0.020	1.2	2.1	3.4
29	CH_3	NH	H	4-hydroxyphenyl	0.27	0.64	0.012	0.015	2.1	2.7	4.05

[a-c] See footnotes in Table I.

Table V. Effect of Combining Substituents in Regions A–D

no.	R^1	R^2	R^3	R^4	*E. coli* K_i,[a] μM		human K_i,[a] μM		IC_{50},[b] μM		
					K_{is}	K_{ii}	K_{is}	K_{ii}	L1210	CCRF-CEM	GC_3/M TK⁻
30	CH_3	O	H	phenyl	>1[c]	>1[c]	0.83	0.71	4.2	3.5	>5.0[c]
31	H	O	CH_3	phenyl	>1[c]	>1[c]	1.0	1.1	2.0	2.5	>5.0[c]
32	CH_3	O	CH_3	4-methoxyphenyl	5.0	5.6	0.064	0.094	2.0	4.0	>5.0[c]
33	CH_3	NH	CH_3	4-methoxyphenyl	1.3	1.4	0.048	0.032	0.31	0.4	0.97
34	CH_3	O	CH_3	morpholinyl	1.4	1.0	0.076	0.039	2.6	3.9	>5.0[c]
35	CH_3	NOH	CH_3	4-methoxyphenyl	1.1	0.87	0.043	0.10	4.1	5.0	>10.0[c]
36	CH_3	NCH_3	CH_3	4-methoxyphenyl	0.51	1.0	0.039	0.029	0.72	0.89	1.5
37	CH_3	SCH_3	H	4-hydroxyphenyl	22	16	3.8	2.9	>4.0[c]	>4.0[c]	>4.0[c]
38	CH_3	NH	CH_3	morpholinyl	0.13	0.18	0.020	0.015	0.22	0.22	0.44
39	CH_3	O	CH_3	4-nitrophenyl	2.7	2.6	0.13	0.12	0.89	2.4	>5.0[c]
40	CH_3	O	CH_3	4-aminophenyl	1.3	1.8	0.046	0.039	3.3	5.0	>5.0[c]
41	CH_3	NH	CH_3	4-nitrophenyl	1.1	2.0	0.090	0.064	0.57	0.69	0.91
42	CH_3	NH	CH_3	4-aminophenyl	0.30	0.53	0.043	0.030	0.28	0.2	0.27
43	CH_3	NCH_3	CH_3	morpholinyl	0.055	0.088	0.021	0.013	0.18	0.61	0.21
44	CH_3	NCH_3	H	morpholinyl	1.3	6.3	0.017	0.053	1.8	>5[c]	>5[c]

[a-c] See footnotes in Table I.

carbonyl, and in addition, create a Coulombic interaction with Asp 169. The crystal structure of amidine 12 bound in the *E. coli* TS active site is consistent with this analysis.[10] We were not able to obtain a crystal structure of *N*-methyl amidine 15, but there appears to be room to accommodate the methyl group by placing it away from the Ala 263 carbonyl, allowing the NH to make the favorable hydrogen bond with the carbonyl oxygen of Ala 263.

The third area we investigated was the 5-position of the benzindole ring, region C. In Figure 2, a small cavity is apparent between the 5-carbon and Trp 80. We felt that a small hydrophobic substituent would fill this space well and have favorable van der Waals interactions with the tryptophan. Such a substituent, in addition to filling extra space, would serve to lock the N-6 dialkyl substituent perpendicular to the plane of the benzindole ring as is commonly seen with peri-substituted naphthalenes.[14] Since this conformation is seen in the enzyme inhibitor crystal structures, the restriction on conformational flexibility introduced by C-5 substituents should improve binding on entropic grounds. In addition, changes in the electronic properties of a 5-substituent could be used to optimize the pK_a of the amidine-containing inhibitors. Three different substituents were investigated, and of these (shown in Table III), the methyl group in compound 16 conferred the largest increase in inhibition. Compare, for

(14) Balasubramaniyan, V. Peri Interactions in Naphthalene Derivatives. *Chem. Rev.* **1966**, *66*, 567–641.

example, compounds **16** and **30** (see Table V). In this case the methyl increased inhibition against the human enzyme by a factor of 10. In the case of the 5-chloro substituent, comparison of compounds **18** and **25** (see Table V) reveals this substituent to increase inhibition by only a factor of 2. However, for amidine **17**, the degree of increased inhibition over the desmethyl compound **12** was large for the *E. coli* enzyme but negligible for the human enzyme. The implication of these results is that the binding modes of the amidines for the two enzymes are not identical. Morphological and or electrostatic differences in this region of the two sites could be the cause, but without the human crystal structure, these inconsistencies are difficult to rationalize.

The last area investigated as an independent variable was region D. The piperazinyl substituent, first used in compound **3**, was used primarily for solubility purposes. Since the inhibition of the initial compound in a novel series cannot be predicted, a solubilizing functional group was used to ensure success in the protein crystallization experiments. Once these objectives had been achieved and potency had been improved, the piperazinyl group was replaced with other substituents. One characteristic feature of this portion of the protein, as can be seen in Figure 3, is that substituents in this area protrude out of the active site into bulk solvent. In addition, the only area of contact between this portion of the ligand and the protein is a relatively flat hydrophobic wall created by the side chain of Ile 79. The result of this should therefore be only modest changes in binding affinity from one compound to the next. As is shown in Table IV, both aromatic and heteroalkyl groups were tested. The results are consistent with the above analysis. The unsubstituted phenyl group in compound **21** and the piperazinyl group in compound **3** show similar K_is. The para-substituted phenyl sulfones **22–24**, **26**, **28**, and **29** were prepared in order to investigate the electronic requirements of this region of the protein. The results indicate that there is a small preference for electron-donating groups over electron-withdrawing groups but again this is not large. The morpholinyl moiety in compounds **25** and **27** show a slight improvement in K_i roughly equal to the substituted phenyl groups. Although large increases in binding energy were not expected from changes in this part of the molecule, substituents in this region did turn out to modulate target selectivity and pharmacological properties (see the Discussion section).

What remained was to combine the optimal substituents from each of the four regions. The results of these experiments are shown in Table V. Clearly, all four variables are not completely independent of each other, but some general trends in activity can be seen. For example in region A, the methyl group at N-6 shows similar increases in activity over the ethyl group regardless of changes in regions B–D. This is exemplified by comparing lactams **3** and **9** with amidines **11** and **12**. In addition, the amidine-containing compounds in region B are in general more active than the lactam-containing compounds, but the relative magnitude is dependent on the type of substituent in region C. For example, comparison of compounds **12** and **30** reveals that the amidine is worth a factor of 20 in binding against the human enzyme. However, in compounds **16** and **17**, where the C-5 substituent is now a methyl group, the lactam to amidine change is only worth a factor of 2 in increased inhibitory activity. Region D, as expected from the nature of its minimal interactions with the protein, appears to be an independent variable.

Chemistry

The synthesis of lactam **3** is shown in Scheme I. The

Scheme I[a]

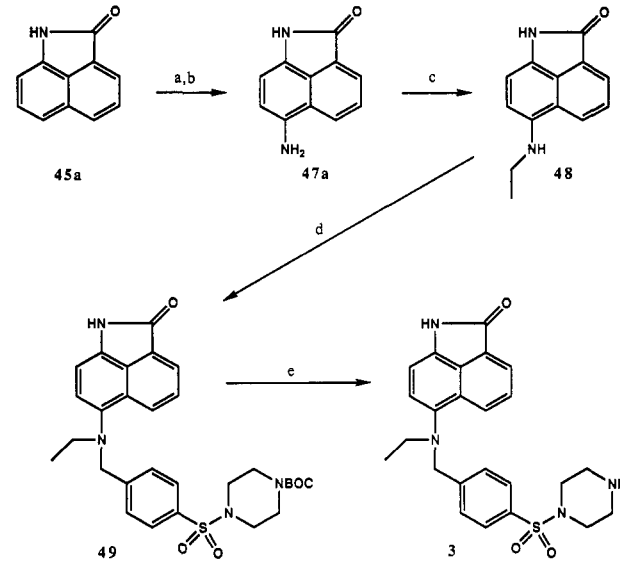

[a] (a) HNO_3, HOAc, (85%); (b) H_2, Pd/C, THF, (77%); (c) EtI, K_2CO_3, DMF, (61%); (d) **55**, K_2CO_3, DMF, (47%); (e) HCl, MeOH, (94%).

Scheme II[a]

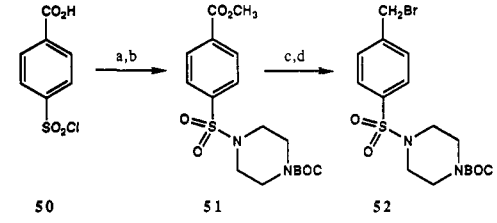

[a] (a) *t*-BOC-piperazine, diisopropylethylamine, THF, (53%); (b) MeI, K_2CO_3, DMF (91%); (c) DIBAL, THF, (93%); (d) CBr_4, Ph_3P, CH_2Cl_2 (96%).

synthesis begins with the nitration of commercially available benz[*cd*]indol-2(1*H*)-one (**45a**)[15] to yield the known 6-nitrobenz[*cd*]indol-2(1*H*)-one (**46a**).[16] Reduction of the nitro group gives the key intermediate aniline **47a** in 77% yield. Selective monoalkylation of the aniline nitrogen with ethyl iodide provided **48** in 61% yield. Benzylation with bromide **52** and subsequent deprotection provided **3**.

For the preparation of bromide **52** we initially attempted to brominate the tosylated *t*-BOC-piperazine using NBS under free-radical conditions.[17] This method provided only trace amounts of the desired product. An alternative route was devised and that is shown in Scheme II. Treatment of 4-(chlorosulfonyl)benzoic acid with *t*-BOC-piperazine and base followed by methylation[18] provided methyl ester **51** in a combined yield of 48%. DIBAL reduction in THF and bromination with triphenylphosphine

(15) Purchased from the Aldrich Chemical Company, Inc., Milwaukee, WI.

(16) Corbellini, A.; Atti, M.; Fossati, V. Anthanthrones and Derivatives. IV. Synthesis of Substituted Anthanthrones. *Rend. Ist. Lomb. Sci. Lett., B* **1936**, *69*, 287–299; *Chem. Abstr. 33*, 6291.[8]

(17) Mataka, S.; Kurisu, M.; Takahashi, K.; Tashiro, M. Bromination of Methyl Substituted 1,2,5-Thiadiazoles With N-Bromosuccinimide. *J. Heterocycl. Chem.* **1984**, *21*, 1157–1160.

(18) Pfeffer, P. E.; Silbert, L. S. Esterification of Alkylation of Carboxylate Salts. Influence of Steric Factors and Other Parameters on Reaction Rates. *J. Org. Chem.* **1976**, *41*, 1373–1379.

Scheme III.[a] General Synthesis of Lactam-Containing Inhibitors

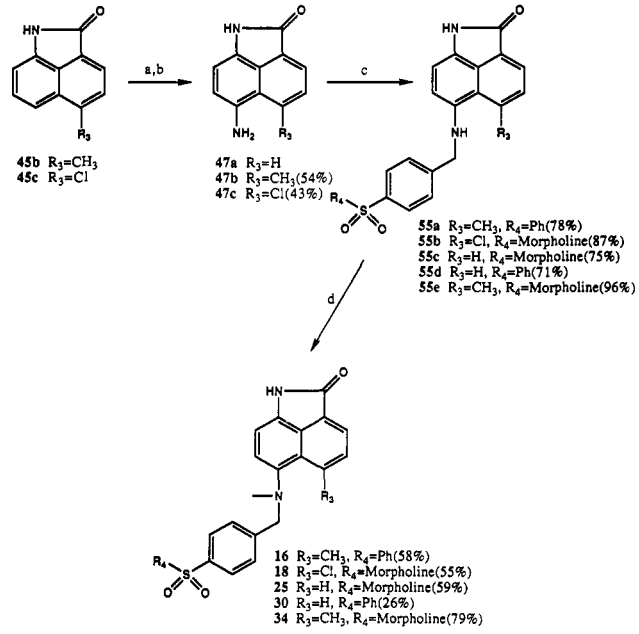

[a] (a) HNO_3, HOAc, H_2SO_4; (b) $SnCl_2$, EtOH or Ra(Ni), N_2H_4, THF; (c) benzyl bromide, diisopropylethylamine, DMF; (d) CH_3I, diisopropylethylamine, DMF.

Scheme IV.[a] Synthesis of 5-Methylbenz[*cd*]indol-2(1*H*)-one

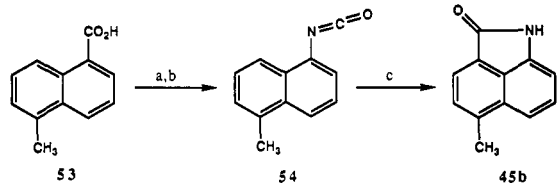

[a] (a) EtOCOCl, acetone, −5 °C, NaN_3, H_2O, −5 °C (82%); (b) ClPh, 132 °C; (c) BCl_3, 110 °C, (51%).

and carbon tetrabromide[19] completed the synthesis in 89% over the two steps.

Many of the dialkylated anilines in Tables I–V were prepared by first alkylating with the benzylic substituent followed by the smaller alkyl group. This method, in some cases, provided better yields of monoalkylated products compared to alkylation with the smaller alkyl group first. This general route to the lactam-containing inhibitors is shown in Scheme III for a few selected compounds. The substituted benz[*cd*]indole anilines **47a–c** were monoalkylated with the corresponding benzylic bromides **62a** or **62b** in DMF using diisopropylethylamine as base. The corresponding anilines **55a–e** were methylated with methyl iodide in DMF and base to complete the synthesis. Low temperatures and short reaction times in the methylation step were critical to prevent dealkylative benzylic cleavage presumably caused by the increasing concentrations of free iodide ion in the reaction mixture.

The two required 5-substituted benz[*cd*]indoles **45b,c** were synthesized via two separate routes. The first, 5-methylbenz[*cd*]indol-2(1*H*)-one (**45b**), was synthesized by the novel route shown in Scheme IV. The key step is the Lewis acid catalyzed cyclization of an isocyanate across the 1- and 8-position of the naphthalene ring to form the

Scheme V[a]

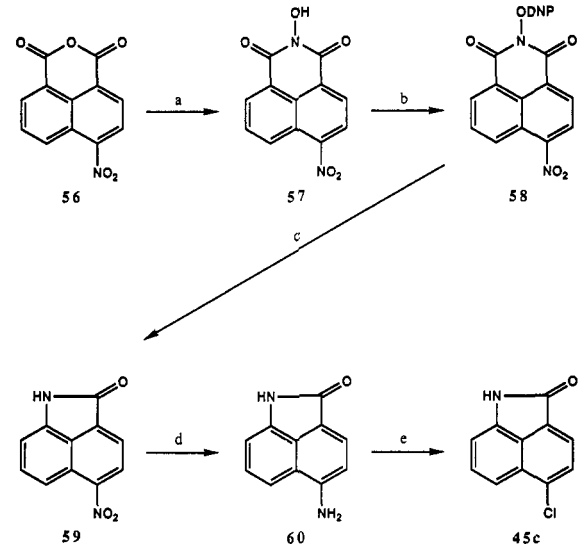

[a] (a) NH_2OH·HCl, NaOAc, H_2O (quant.); (b) 2,4-dinitrochlorobenzene, Na_2CO_3, H_2O (94%); (c) NaOH, EtOH, H_2O (55%); (d) H_2, Raney Ni, THF (76%); (e) *tert*-Butyl nitrite, $CuCl_2$, CH_3CN (94%).

Scheme VI[a]

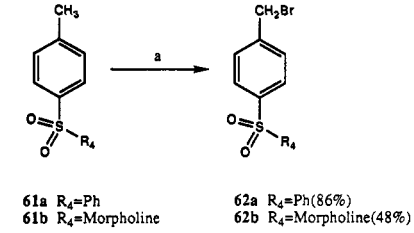

[a] (a) NBS, light, CCl_4.

lactam. In the event, the acyl azide of 5-methylnaphthoic acid[20] was prepared from the corresponding acid by the mixed carbonate anhydride method[21] in 82% yield and rearranged to isocyanate **54** in boiling toluene. Initially, we attempted unsuccessfully to close the ring thermally.[22] A number of Lewis acids were then tried ($AlCl_3$, $TiCl_4$, $AlBr_3$, $SnCl_4$) and eventually it was found that the isocyanate could be cyclized to the desired 5-methylbenz[*cd*]indole **45b** with BCl_3 at 110–115 °C for 28 h in 51% yield from the acyl azide. The generality of this method for the synthesis of substituted benz[*cd*]indol-2(1*H*)-ones is currently being investigated.

5-Chlorobenz[*cd*]indol-2(1*H*)-one (**45c**) could not be constructed as described above and was therefore synthesized as shown in Scheme V. Commercially available 4-nitro-1,8-naphthalic anhydride (**56**)[14] was treated with hydroxylamine to form imidate **57** in quantitative yield. Alkylation with 2,4-dinitrochlorobenzene in aqueous Na_2CO_3 provided compound **58** in excellent yield. Rearrangement of the imidate to the lactam was accomplished with ethanolic NaOH to give 5-nitrobenz[*cd*]indol-2-(1*H*)-one (**59**) contaminated with 15% of the corresponding 6-isomer. A similar method has been previously reported

(19) Kocienski, P. J.; Cernigliaro, G.; Feldstein, G. A Synthesis of (±)-Methyl *n*-Tetradeca-*trans*-2,4,5-trienoate, an Allenic Ester Produced by the Male Dried Bean Beetle *Acanthoscelides obtectus* (Say). *J. Org. Chem.* **1977**, *42*, 353–355.

(20) Fischer, A.; Mitchell, W. J.; Packer, J.; Topsom, R. D.; Vaughan, J. Dissociation Constants of Some Methylnaphthoic and Acenaphthoic Acids. *J. Chem. Soc.* **1963**, 2892–2896.

(21) Weinstock, J. A Modified Curtius Reaction. *J. Org. Chem.* **1961**, *26*, 3511.

(22) Cyclizations of this type have been used in the synthesis of bicyclic carbostyrils. Eloy, F.; Deryckere, A. Synthesis of Isocarbostyrils and 1-Chloroisoquinolines. *Helv. Chim. Acta* **1969**, *52*, 1755–1762.

Scheme VII.[a] General Synthesis of Amidine-Containing Inhibitors

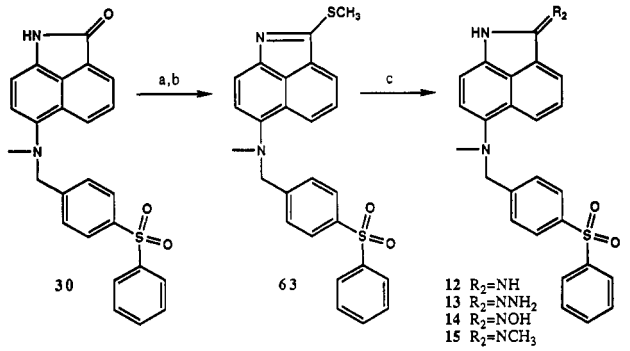

[a] (a) Lawesson's reagent, toluene, (47%); (b) CH_3I, NaOH, THF, EtOH, (95%); (c) MeOH, NH_3 → **12**, (87%); N_2H_4 → **13**, (87%); NH_2OH → **14**, (84%); NH_2CH_3 → **15**, (75%).

to give pure **59**,[23] a result we have been unable to reproduce. Reduction to aniline **60** followed by diazotization and chlorination with *tert*-butyl nitrite and cupric chloride[24] completes the synthesis. It is worth mentioning that the synthesis of compound **45c** via rearrangement of the corresponding alkylated imidate is described in the same account as nitrobenzindole **59**.[23] However, again in attempts to reproduce the described procedure, we obtained an inseparable 1:1 mixture of the 5- and 6-chloro isomers.

With the exception of bromide **52**, all of the required benzylic bromides **62** were prepared by radical bromination[17] of the appropriately substituted 4-methyl sulfones **61** as shown in Scheme VI. The yields were in general moderate, often giving inseparable mixtures of monobrominated and dibrominated products along with starting material. However, these mixtures were suitable for use in the alkylation step as the dibromide and starting toluene were unreactive.

A general procedure for converting the lactam function in the benz[*cd*]indol-2(1*H*)-one series into the substituted amidine function is shown in Scheme VII. The lactams were first converted to the thiolactams with Lawesson's reagent[25] in moderate to good yields. The corresponding thiolactams were alkylated with methyl iodide[26] to give intermediates **63** in excellent yield. The thiomethyl group was displaced with the appropriately substituted amine[27] in methanol in a sealed tube to give the final compounds **12–15**.

Biochemistry and Biology

The compounds shown in Tables I–V were evaluated for their inhibition of both purified recombinant *E. coli* and human thymidylate synthase. The observed inhibition patterns relative to the cofactor 5,10-methylenetetrahydrofolate were dominantly mixed noncompetitive or noncompetitive. Consequently, both K_{is} and K_{ii} values are reported.[28] The fact that the compounds are known to bind at the folate site and yet are noncompetitive with the folate cofactor is an interesting and as yet unexplained observation. We have however observed this property with other folate site TS inhibitors such as compound **2**[10] and are continuing to investigate its cause.

Table VI. Effect on IC_{50} of 10 μM Thymidine

no.	human K_i,[a] μM K_{is}	human K_i,[a] μM K_{ii}	IC_{50},[b] μM, L1210	thymidine shift[c]
3	3.0	1.6	6.0	1.1
17	0.035	0.044	0.25	3.85
19	0.029	0.020	0.44	5.5
27	0.012	0.015	0.49	6.7
38	0.020	0.015	0.22	12
43	0.021	0.013	0.18	10.6

[a–b] See footnotes in Table I. [c] Expressed as the ratio of the IC_{50} in the presence of 10 μM thymidine divided by the IC_{50} with no thymidine added. See Experimental Section for a detailed description.

The compounds were also assayed for their cell growth inhibition against three standard tumor cell lines: L1210 murine leukemia; CCRF-CEM, a human lymphoblastic leukemia line of T-cell origin; and GC_3/M TK^-, a human thymidine kinase deficient adenocarcinoma line. Results are reported as IC_{50} values (in μM).[28]

To assess whether TS is the target of cell growth inhibition, all compounds were tested against L1210 in the presence of 10 μM thymidine. A shift of the IC_{50} to a larger number is considered a positive result in that cells are protected from cell death by salvaging the exogenous thymidine. What we found was that most compounds that were moderate inhibitors of human TS, i.e. above 40 nM, showed very little shift in the IC_{50} curves in the presence of exogenous thymidine, indicating some degree of nonspecific binding to other targets. Many inhibitors did however show increased reversal effects (implying selectivity for TS) with increased potency against the human enzyme. That is, in general, the most potent inhibitors of human TS showed the largest shift in IC_{50} with the addition of thymidine. Table VI shows the results of the thymidine shift experiments for a select number of compounds from this series. The data is presented as the ratio of IC_{50} values with and without 10 μM thymidine. In the cases where no shift in the IC_{50} was observed, the identities of the alternate cellular targets are not yet known.[29]

Discussion

During the course of these studies, 41 analogues of the lead compound **3** were synthesized and evaluated for biological activity. Based on the crystal structure of **3** bound in *E. coli* TS, four areas for elaboration were identified. Each area was independently optimized, and finally, the best substituents in each region were combined to yield compounds with substantial improvements in binding. Inhibition constants for all derivatives were measured for

(23) Plakidin, V. L.; Vostrova, V. N.; Gnatyuk, P. P.; Zadorozhnyi, N. M. Naphthalic Acid Derivatives XI. General Preparative Method for the Production of Derivatives of 1H-Benzo[c,d]-indol-2-one by the Reaction of N-(2,4-Dinitrophenoxy)-Naphthalimide with Alkalis. *Zh. Org. Khim.* **1977**, *13*, 2194–2202.

(24) Doyle, M. P.; Siegfried, B.; Dellaria, J. F. Alkyl Nitrite-Metal Deamination Reactions. 2. Substitutive Deamination of Arylamines by Alkyl Nitrites and Copper(II) Halides. A Direct and Remarkably Efficient Conversion of Arylamines to Aryl Halides. *J. Org. Chem.* **1977**, *42*, 2426–2431.

(25) Pedersen, B. S.; Scheibye, S.; Nilsson, N. H.; Lawesson, S.-O. Studies on Organophosphorus Compounds. XX Syntheses of Thioketones. *Bull. Soc. Chim. Belg.* **1978**, *87*, 223.

(26) Ficken, G. E.; Kendall, J. D. The Reactivity of the Alkylthio-Group in Nitrogen Ring Compounds. Part III. 2-Methylthiobenz[cd]indole and its Methiodide. *J. Chem. Soc.* **1960**, 1537.

(27) Kroger, M.; Cramer, F. *Liebigs Ann. Chem.* **1977**, 1668–1675.

(28) See Experimental Section for details of these assays.

(29) In vitro reversal of cytotoxicity experiments with leucovorin and hypoxanthine individually and in combination have been run for a number of the compounds in Tables I–V. Compounds **27** and **43**, which do reverse with thymidine, do not show additional effects with leucovorin or hypoxanthine. Compounds **12**, **40**, and **42**, which show no reversal with thymidine, also did not show reversal effects with leucovorin or hypoxanthine. The results of these experiments imply that neither GAR transformylase nor DHFR are likely sites of cytotoxicity.

both *E. coli* and human TS, and the two sources of inhibition data were useful as design guides for somewhat different reasons. Crystallographic work was performed exclusively with the *E. coli* TS and consequently inhibition of this enzyme was used to track the results of inhibitor design. Since the overall goal however was to obtain a human antitumor compound, inhibition of human TS was the primary concern. As it turned out, most changes that improved *E. coli* binding also improved human binding and by roughly the same magnitude. This of course is reassuring in that it indicates that the compounds have similar binding modes in both enzymes which therefore reinforces the correlation that can be made between the *E. coli* enzyme crystal structure and the human enzyme K_i.

As can be seen in Tables I–V, compounds **3–44** have human TS inhibition constants ranging from 13 μM to 12 nM. Analysis of the results in this SAR study leads to the following conclusions. In region A, a smaller alkyl substituent such as methyl or a larger one with a terminal hydroxyl group are roughly 3–4 times better an enzyme inhibitor than the lead. This variable appears to be independent of other changes in the molecule. In region B, the amidines are always more active than the lactams with the unsubstituted amino usually being the best. The relative magnitude of this difference is however dependent on the substituent in region C. Changes in region D demonstrate that the morpholinyl and substituted aromatic groups are most preferred, although only slightly, and that again this variable is principally independent of changes elsewhere in the molecule. The variable that is the least independent is region C. Although hydrogen and methyl are better than chloro and methylthio, distinction between these two is dependent on whether region B is a lactam or an amidine. This is particularly true for the human enzyme. The results of combining the best substituents from the various regions leads to the very potent human TS inhibitors **27** (K_{is} = 12 nM), **29** (K_{is} = 12 nM), **38** (K_{is} = 20 nM), **43** (K_{is} = 21 nM), and **44** (K_{is} = 17 nM).[30]

The in vitro results presented in Tables I–V show that many of the compounds in this series have significant cytotoxic effects, with L1210 IC_{50}'s of less than 1 μM. The most active of these are compounds **27** (0.49 μM), **38** (0.22 μM), **42** (0.28 μM), and **43** (0.18 μM). The K_i/IC_{50} ratio of these compounds range from 0.02 to 0.12, indicating that a significant proportion of the compounds are crossing the cell membranes by what is presumable passive diffusion. This ratio of K_i/IC_{50} is in the range of other known glutamate-containing TS inhibitors which require active transport.[10] Of these, as shown in Table VI, all but one display significant reversal of cytotoxicity with addition of 10 μM thymidine. It is comforting to note that in general the best human TS inhibitors, **27**, **38**, and **43**, are also the most cytotoxic agents in cell culture and that this is due to TS inhibition.

Assuming that the thymidine shift experiments are an accurate measure of TS targeting, a significant conclusion about one of our underlying assumptions can be drawn from this study. That is that the structure-based design of small molecule inhibitors to TS, *and possibly to other targets as well*, does not ensure target selectivity in cells. Instead we see that selectivity, although obtainable, requires very potent inhibitors (K_i's < 20 nM). Moderate inhibitors were either not cytotoxic or were cytotoxic for reasons not relating to TS inhibition.

(30) Tight-binding kinetics as described by Henderson (Henderson, P. J. F. A Linear Equation that Describes the Steady-State Kinetics of Enzymes and Subcellular Particles Interacting with Tightly Bound Inhibitors. *Biochem. J.* **1972**, *127*, 321) have been run on compound **27** against human TS. The inhibition was observed to be noncompetitive with $K_{is} = K_{ii}$ = 2.0 nM. The full details of this study will be published elsewhere.

Conclusion

We have investigated the structure–activity relationships of the de novo designed lead compound **3** using the crystal structure of the *E. coli* complex as a primary guide for design. The SAR study was based on the assumption that the four regions identified from the original crystal structure as suitable for modification could be optimized independently and finally combined to obtain the best inhibitors. Results show this modular approach to structure–activity relationships to be legitimate when structural information about the mode of binding is available. Using this method the inhibition of the human TS was improved from the lead compound by a factor of 500. In vitro antitumor studies showed that many of the compounds had significant cytotoxicity and thymidine shift experiments demonstrated this to be due to TS inhibition.

Experimental Section

Proton magnetic resonance spectra were determined using a General Electric QE-300 spectrometer operating at a field strength of 300 MHz. Chemical shifts are reported in parts per million (δ) and setting the references such that in $CDCl_3$ the $CHCl_3$ is at 7.26 ppm and in DMSO-d_6 the DMSO is at 2.49 ppm. Standard and peak multiplicities are designated as follows: s, singlet; d, doublet; dd, doublet of doublets; t, triplet; brs, broad singlet; brd, broad doublet; br, broad signal; m, multiplet. Mass spectra were determined at either the University of California Riverside or the University of California Berkeley Mass Spectrometry Centers. Infrared absorption spectra were taken on either a Perkin-Elmer 457 spectrometer or a MIDAC Corporation FTIR. Elemental microanalyses were performed by Atlantic Microlab Inc. (Norcross, GA) or MHW Laboratories (Phoenix, AZ) and gave results for the elements stated within ±0.4% of the theoretical values. *N-N*-Dimethylformamide (DMF) was dried over activated (250 °C) 4-Å molecular sieves; *N,N*-dimethylacetamide (DMA) (Aldrich Gold Label grade) was similarly dried. Tetrahydrofuran (THF) was distilled from sodium benzophenone ketyl under nitrogen. Ether refers to diethyl ether. Pet. ether refers to petroleum ether of bp 36–53 °C. Flash chromatography was performed using Silica gel 60 (Merck Art 9385). Thin-layer chromatography (TLC) was performed on precoated sheets of silica 60 F_{254} (Merck Art 5719). Melting points were determined on a Mel-Temp apparatus and are uncorrected.

Measurement of Tissue Culture IC_{50}'s. IC_{50} values for the inhibition of cellular growth were measured using a modification[32] of the MTT[33] colorimetric assay of Mosmann[34] using mouse (L1210) and human (CCRF-CEM) leukemia lines (ATCC) and a human adenocarcinoma (GC_3/M TK^-) deficient in thymidine kinase.[35] Cells were seeded at 1000 (L1210) or 10 000 (CCRF-CEM, GC_3/M TK^-) cells per well in 96-well plates, and growth was measured over a range of nine 2-fold serial dilutions of each compound. Culture medium (RPM1-1640) contained 5% (L1210, CCRF-CEM) or 10% (GC_3/M TK^-) fetal calf serum and 0.5%

(31) Lomax, M. I. S.; Greenberg, G. R. A New Assay of Thymidylate Synthetase Activity Based on the Release of Tritium from Deoxyuridylate-5-3H. *J. Biol. Chem.* **1967**, *242*, 109.
(32) Alley, M. C.; Scuderio, D. A.; Monks, A.; Hursey, M. L.; Czerwinski, M. J.; Fine, D. L.; Abbott, B. J.; Mayo, J. G.; Schoemaker, R. H.; Boyd, M. R. Feasibility of Drug Screening with Panels of Human Tumor Cell Lines using a Microculture Tetrazolium Assay. *Cancer Res.* **1988**, *48*, 589.
(33) MTT is 3-(4,5-dimethylthiazol-2-yl)-2,5-diphenyltetrazolium bromide.
(34) Mosmann, T. J. Rapid Colorimetric Assay for Cellular Growth and Survival: Application to Proliferation and Cytotoxicity Assays. *J. Immunol. Methods* **1983**, *65*, 55.
(35) Kindly supplied by Dr. P. J. Houghton and Dr. J. A. Houghton, St. Jude Children's Research Hospital, Memphis, TN.

Table VII. Analytical Data

no.	mp, °C	method[a]	analyses	mass spec	formula
3	150 dec	A	C,H,N,S,Cl		$C_{24}H_{26}N_4O_3S\cdot 2HCl$
4	187–189	A	C,H,N,S		$C_{25}H_{28}N_4O_3S$
5	oil	A	C,H,N,S	exact	$C_{25}H_{28}N_4O_3S\cdot 0.6H_2O$
6	98 dec	A	C,H,N[b]	exact	$C_{24}H_{26}N_4O_4S\cdot 2.1MeOH$
7	178–179	A	C,H,N,S	exact	$C_{25}H_{28}N_4O_4S$
8	170–180 dec	B	C,H,N,S	exact	$C_{26}H_{22}N_2O_3S_2\cdot 0.1H_2O$
9	207–210	B	C,H,N,S	exact	$C_{23}H_{24}N_4O_3S\cdot$maleate
10	256–260 dec	B	C,H,N,S		$C_{24}H_{18}N_2O_3S$
11	oil	A	C,H,N,S	exact	$C_{26}H_{23}N_3O_2S\cdot 1.7H_2O$
12	120–130 dec	B	C,H,N,S	exact	$C_{25}H_{21}N_3O_2S\cdot 2.6H_2O$
13	160 dec	B	C,H,N,S	exact	$C_{25}H_{22}N_4O_2S\cdot 0.2N_2H_4\cdot 0.2H_2O$
14	185 dec	B	C,H,N,S	exact	$C_{25}H_{21}N_3O_3S$
15	221–223	B	C,H,N,S	exact	$C_{26}H_{23}N_3O_2S$
16	202–204	B	C,H,N,S	exact	$C_{26}H_{22}N_2O_3S$
17	145 dec	B	C,H,N,S	exact	$C_{26}H_{23}N_3O_2S\cdot H_2O$
18	266–268	B	C,H,N,S,Cl	exact	$C_{23}H_{22}ClN_3O_4S$
19	228–230	B	C,H,N,S,Cl	exact	$C_{23}H_{23}ClN_4O_3S$
20	224–225	B	C,H,N,S	exact	$C_{24}H_{27}N_4O_3S_2$
21	213–216	A	C,H,N,S	exact	$C_{26}H_{22}N_2O_3S\cdot 0.5H_2O$
22	107 dec	B	C,H,N,S,Cl	exact	$C_{25}H_{21}ClN_2O_4S\cdot 0.7H_2O$
23	180–182	B	C,H,N,S		$C_{26}H_{22}N_2O_4S$
24	140 dec	B	C,H,N,S	exact	$C_{25}H_{21}N_3O_3S\cdot CH_2Cl_2$
25	200–202	B	C,H,N,S	exact	$C_{23}H_{23}N_3O_4S$
26	197–200	B	C,H,N,S	exact	$C_{25}H_{19}N_3O_5S\cdot 0.5H_2O$
27	180 dec	B	C,H,N,S	exact	$C_{23}H_{24}N_4O_3S\cdot 0.5C_6H_6 0.5H_2O$
28	208–209	B	C,H,N,S		$C_{26}H_{23}N_3O_3S$
29	oil	B	C,H,N,S	exact	$C_{25}H_{21}N_3O_3S\cdot 0.5AcOH\cdot 1.7H_2O$
30	228–230	B	C,H,N,S	exact	$C_{25}H_{20}N_2O_3S$
31	310 dec	B	C,H,N,S	exact	$C_{25}H_{20}N_2O_3S\cdot 0.75H_2O$
32	222–223	B	C,H,N,S	exact	$C_{27}H_{24}N_2O_4S$
33	135 dec	B	C,H,N,S	exact	$C_{27}H_{25}N_3O_3S\cdot 0.5H_2O$
34	266–267	B	C,H,N,S	exact	$C_{24}H_{25}N_3O_4S\cdot 0.5H_2O$
35	135 dec	B	C,H,N,S	exact	$C_{27}H_{25}N_3O_4S$
36	243–245 dec	B	C,H,N,S	exact	$C_{28}H_{27}N_3O_3S$
37	83 dec	B	C,H,N	exact	$C_{26}H_{22}N_2O_3S_2\cdot 2.1H_2O$
38	210 dec	B	C,H,N,S		$C_{24}H_{26}N_4O_3S\cdot$maleate
39	225 dec	B	C,H,N,S	exact	$C_{26}H_{21}N_3O_5S\cdot 0.25H_2O$
40	222–226	B	C,H,N,S	exact	$C_{26}H_{23}N_3O_3S\cdot 0.25H_2O$
41	95 dec	B	C,H,N,S	exact	$C_{26}H_{22}N_4O_4S\cdot 1.3AcOH\cdot 1.75H_2O$
42	95 dec	B	C,H,N,S	exact	$C_{26}H_{24}N_4O_2S\cdot 2.0AcOH\cdot 2.2H_2O$
43	270 dec	B	C,H,N,S	exact	$C_{25}H_{28}N_4O_3S$
44	190 dec	B	C,H,N,S		$C_{24}H_{26}N_4O_3S\cdot$maleate$\cdot 0.5H_2O$

[a] The method refers to the order in which the alkyl groups were introduced onto the N-6 nitrogen. In method A, the smaller alkyl group was introduced first as in Scheme I. In method B, the benzylic group was introduced first as in Scheme III. [b] Calcd for $C_{24}H_{26}N_4O_4S\cdot 2.1MeOH$: C, 58.72; H, 6.50; N, 10.50. Found: C, 59.09; H, 6.04; N, 10.10.

DMSO. Following a 3 day (L1210) or 5 day (CCRF-CEM, GC_3/M TK^-) incubation and a 4-h treatment with MTT, cells were harvested, and growth was measured spectrophotometrically after dissolution of the deposited formazan in DMSO. IC_{50} values were determined from semilogarithmic plots of compound concentration vs the mean of the four growth assessments made at each serial dilution of the agent relative to the growth of control cultures.

Measurement of IC_{50} Shift Due to Thymidine. The ability of thymidine to reverse growth inhibition was assessed by comparing the IC_{50} measured under standard conditions (RPM1-1640 medium containing 5% fetal calf serum) with that obtained in the presence of 10 μM thymidine which was replenished daily during the 3 days of growth. The magnitude of the ratio of the IC_{50} measured in the presence of thymidine to that measured without added nucleoside was used to reflect the extent to which the inhibition of growth could be attributed to intracellular inhibition of thymidylate synthase. A value of 1.0 under these conditions would reflect a probable locus of action other than TS while larger values probably reflect a direct relationship between growth inhibition and TS targeting.

Biochemical Assays. TS activity was assayed by a modified procedure of the tritium release method of Lomax and Greenberg.[31] Inhibition constants were determined by steady-state analysis against the cofactor 5,10-methylenetetrahydrofolate as the variable substrate under conditions of saturating dUMP. Reaction conditions in 0.1 mL were 50 mM Tris at pH 7.6, 10 mM dithiothreitol, 1 mM ethylenediaminetetraacetic acid, 25 mM $MgCl_2$, 15 mM formaldehyde, 25 μM dUMP ([5-^{3}H], specific activity ≅ 2×10^8 cpm/μmol), and tetrahydrofolate (eight concentrations ranging from 5 to 150 μM). Bovine serum albumin at up to 100 μg/mL was present when human TS was assayed. These reactions were either in the absence of inhibitor or in the presence of inhibitor at concentrations ranging, at a minimum, between $0.5K_i$ and $2.0K_i$ except when the solubility of the inhibitor was limiting. Reactions were run at room temperature by initiating with the addition of enzyme. After 5 min, the reactions were quenched by the addition of charcoal and centrifuged to remove unreacted dUMP, and the supernatant was counted to determine the release of tritium from the 5-position of dUMP. Experimental results were analyzed by a nonlinear regression analysis program[36] which fit the data to a mixed noncompetitive inhibition scheme.

6-Nitrobenz[*cd*]indol-2(1*H*)-one (46a). To a mixture of 33.9 g (0.200 mol) of benz[*cd*]indol-2(1*H*)-one (**45a**) in 150 mL of glacial acetic acid was added dropwise 16.5 mL (0.260 mol) of 70% nitric acid. Over the course of 1 h, the reaction temperature rose to 50 °C. The reaction mixture was cooled to room temperature and a very thick dark green paste resulted. This mixture was filtered, washed with 50% aqueous acetic acid, and dried. The solid was refluxed in 600 mL of MeOH and then cooled to 0 °C. The mixture was filtered, washed with cold MeOH, and dried in vacuo to yield 22.2 g (51%) of 6-nitrobenz[*cd*]indol-2(1*H*)-one. An analytically pure sample was obtained by refluxing 10.52 g of 6-nitrobenz[*cd*]indol-2(1*H*)-one in 350 mL of THF. After refluxing

(36) Perrella, F. W. EZ-FIT, Perrella Scientific, Springfield, PA, 1989.

for 30 min, the mix was filtered, and the filtrate evaporated. The wet solid was stirred in 200 mL of MeOH and the MeOH evaporated. The MeOH slurry and evaporation was repeated. Finally, the solid was taken up in 200 mL of MeOH, heated to reflux, and cooled at −4 °C overnight. The resulting solid was filtered, washed with cold MeOH, and dried in vacuo to yield 8.97 g (85%) of an orange solid. Mp: 298–300 °C [lit. (*Chem. Abstr. 33*, 6291) mp 297–298 °C]. IR (KBr): 3316, 1724, 1638, 1491, 1351, 1252, 1051, 752 cm^{-1}; ^1H NMR (DMSO-d_6/TMS) δ (ppm): 7.10 (d, 1 H, J = 9 Hz), 8.05 (dd, 1 H, J = 6 Hz), 8.16 (d, 1 H, J = 6 Hz), 8.61 (d, 1 H, J = 6 Hz), 8.85 (d, 1 H, J = 9 Hz).

6-Aminobenzo[*cd*]indol-2(1*H*)-one (47a). A solution of 4.00 g (18.7 mmol) of 6-nitrobenz[*cd*]indol-2(1*H*)-one (**46a**) in 300 mL of THF was filtered into a Parr hydrogenation bottle. The insolubles were discarded. To the solution was added 0.44 g of 5% Pd/C, and the mix was put under 40 psi of H_2. After 16 h, the Parr bottle was vented, the reaction mixture filtered through Celite, and the filtrate evaporated. The residue was taken up in hot EtOH, filtered, and then acidified with EtOH saturated with HCl(g). A precipitate formed. To the mix was added dropwise 500 mL of Et_2O. The mix was filtered, washed with Et_2O, and the solid dried in vacuo, yielding 3.44 g of reddish solid. This material was refluxed in 150 mL of EtOH and cooled, and 500 mL of Et_2O added dropwise. The resultant precipitate was collected, washed with Et_2O, and dried in vacuo to yield 3.16 g (77%) of 6-aminobenz[*cd*]indol-2(1*H*)-one hydrochloride. A sample of the free base was prepared by dissolving 1.51 g of the HCl salt in 200 mL of water and basifying the solution with saturated aqueous $NaHCO_3$. A precipitate formed. This was collected, washed with water, and dried in vacuo to yield 1.21 g of (**50a**). Mp: 240–242 °C [lit. (*Chem. Abstr. 33*, 6291) mp 244 °C]. IR (KBr): 3490, 3287, 2905, 1720, 1672, 1647, 1477, 777 cm^{-1}. ^1H NMR (acetone-d_6/TMS) δ (ppm): 2.85 (bs, 2 H), 5.21 (bs, 1 H), 6.64 (d, 1 H, J = 9 Hz), 6.76 (d, 1 H, J = 9 Hz), 7.71 (dd, 1 H, J = 6 Hz), 7.87 (d, 1 H, J = 6 Hz), 8.22 (d, 1 H, J = 6 Hz).

N^6-Ethyl-6-aminobenz[*cd*]indol-2(1*H*)-one Hydrochloride (48). To a mixture of 3.26 g (0.0148 mol) of 6-aminobenz[*cd*]-indol-2(1*H*)-one (**47a**) hydrochloride, 4.18 g (0.0303 mol) of anhydrous K_2CO_3, and 60 mL of DMF was added 1.77 mL (0.0222 mol) of ethyl iodide. This mixture was heated at 70–100 °C for 8 h then cooled to room temperature, diluted with EtOAc, filtered, and evaporated to dryness. This residue was chromatographed on flash silica using $CHCl_3$/MeOH 9:1 as elutant, yielding 2.63 g of crude product. This material was taken up in EtOAc/MeOH and acidified with EtOAc saturated with HCl(g). To this mixture was added dropwise sufficient Et_2O to precipitate the product. The solid was filtered, washed with Et_2O, and dried in vacuo to yield 2.25 g (61%) of **48**. Mp: 261.5–263 °C. IR (KBr): 3490, 1720, 1647, 1478, 777 cm^{-1}. ^1H NMR (DMSO-d_6/TMS) δ (ppm): 1.30 (t, 3 H, J = 6 Hz), 3.36 (q, 2 H, J = 6 Hz), 4.21 (bs, 2 H, NH_2), 6.98 (d, 1 H, J = 9 Hz), 7.35 (bs, 1 H), 7.87 (t, 1 H, J = 6, 9 Hz), 8.08 (d, 1 H, J = 6 Hz), 8.51 (d, 1 H, J = 9 Hz), 10.86 (s, 1 H, NH). Anal. ($C_{13}H_{13}N_2OCl$) C, H, N, Cl.

N^6-Ethyl-N^6-[4-[[4-(*tert*-butoxycarbonyl)piperazinyl]-sulfonyl]benzyl]-6-aminobenz[*cd*]indol-2(1*H*)-one (49). A mixture of 0.371 g (0.619 mmol) of bromide **52**, 0.171 g (1.24 mmol) of anhydrous K_2CO_3, 0.154 g (0.619 mol) of aniline **48**, and 20 mL of DMF was heated at 100 °C until TLC (EtOAc) showed no further reaction. The mixture was cooled to room temperature and added to 100 mL of H_2O. A small amount of saturated aqueous NaCl solution was added to coagulate the solid. The solid was filtered, washed with H_2O, and dried in vacuo, yielding 0.37 g of crude product. This material was dissolved in chloroform and chromatographed on flash silica using EtOAc/hexane 1:1 as elutant to yield 0.16 g (47%) of **52** as a pure glass. ^1H NMR ($CDCl_3$/TMS) δ (ppm): 1.12 (t, 3 H, J = 9 Hz), 1.40 (s, 9 H), 2.95 (m, 4 H), 3.25 (q, 2 H, J = 9 Hz), 3.50 (m, 4 H), 4.43 (s, 2 H), 6.84 (d, 1 H, J = 9 Hz), 6.92 (d, 1 H, J = 9 Hz), 7.54 (d, 2 H, J = 9 Hz), 7.67 (d, 2 H, J = 9 Hz), 7.75 (dd, 1 H, J = 9 Hz), 8.09 (d, 1 H, J = 9 Hz), 8.30 (m, 2 H). A derivative of this compound was characterized in the next step.

N^6-[4-(Piperazinylsulfonyl)benzyl]-6-aminobenz[*cd*]indol-2(1*H*)-one (3). A solution of 0.161 g (0.292 mmol) of compound **49** in 10 mL of MeOH was acidified with MeOH saturated with HCl(g). This solution was stirred at room temperature until TLC (EtOAc) showed lack of starting material. The solvent was evaporated and the residue partitioned between saturated aqueous $NaHCO_3$ solution and $CHCl_3$. The $CHCl_3$ was evaporated and the residue chromatographed on flash silica using $CHCl_3$/MeOH 95:5 as elutant to yield 0.124 g (94%) of **3** as a yellow solid. For analytical purposes, 102 mg of the free base was taken up in 5 mL of EtOAc and acidified with EtOAc saturated with HCl(g). Et_2O was added to precipitate the product. The yellow solid was filtered, washed with Et_2O, and dried in vacuo to yield 92 mg of the HCl salt. Mp: 150 °C dec. IR (KBr): 3439, 2920, 1701, 1644, 1476, 1356, 1163, 945, 735 cm^{-1}. ^1H NMR ($CDCl_3$, TMS) δ (ppm): 1.11 (t, 3 H, J = 9 Hz), 2.93 (m, 8 H), 3.24 (q, 2 H, J = 9 Hz), 4.42 (s, 2 H), 6.86 (d, 1 H, J = 9 Hz), 6.94 (d, 1 H, J = 9 Hz), 7.55 (d, 2 H, J = 9 Hz), 7.67 (d, 2 H, J = 9 Hz), 7.73 (dd, 1 H, J = 6 Hz), 8.09 (d, 1 H, J = 6 Hz), 8.29 (d, 1 H, J = 6 Hz), 8.56 (s, 1 H).

4-(Bromomethyl)phenyl Phenyl Sulfone (62a). To a rapidly stirred solution of 15 g (64.6 mmol) of phenyl *p*-tolyl sulfone in 300 mL of CCl_4 at 85 °C was added 11.5 g (64.6 mmol) of NBS. The mixture was irradiated with a 200-W heat lamp for 30 min. After cooling, the mixture was filtered and the solvent evaporated. The crude residue was chromatographed on flash silica (500 g) with EtOAc/pet. ether (15:85) to yield 17.4 g (86%) of bromide **62a** as a white solid contaminated with about 10% of the corresponding dibromide. Repeated chromatography and recrystallizations failed to remove the contaminate and the material was used in the next step as such. IR (KBr): 1290, 1140, 1100, 720 cm^{-1}. ^1H NMR ($CDCl_3$) δ (ppm): 4.45 (s, 2 H, CH_2Ar), 7.51–7.62 (m, 5 H), 7.90–8.00 (m, 4 H). HRMS: m/e calcd for $C_{13}H_{11}O_2SBr$ 309.9663, found 309.9648.

Methyl 4-[[4-(*tert*-Butoxycarbonyl)piperazinyl]-sulfonyl]benzoate (51). To a rapidly stirred solution of 40 g (215 mmol) of *tert*-butyl 1-piperazinecarboxylate and 18.5 mL (128 mmol) of DIEA in 300 mL of dry THF at 25 °C was added dropwise over a 1-h period a solution of 23.7 g (107 mmol) of 4-(chlorosulfonyl)benzoic acid in 200 mL of dry THF. The resulting mixture was stirred for an additional 1 h and then poured into H_2O (1000 mL). After extraction with EtOAc (300 mL which was discarded), the aqueous layer was acidified to pH 1 with concentrated HCl and then extracted with EtOAc (3 × 1000 mL). The combined organic layers were dried (Na_2SO_4) and the solvent was evaporated to yield 21 g (53%) of the desired 4-[[4-(*tert*-butoxycarbonyl)piperazinyl]sulfonyl]benzoic acid as an off-white solid. ^1H NMR (DMSO-d_6) δ 1.33 (s, 9 H), 2.89 (brs, 4 H), 3.40 (brm, 4 H), 7.86 (d, 2 H, J = 9 Hz), 8.17 (d, 2 H, J = 9 Hz). The methyl ester of this material was fully characterized in the next step.

To a rapidly stirred solution of 21 g (56.7 mmol) of the above acid and 23.5 g (170 mmol) of K_2CO_3 in 300 mL of DMF at 25 °C was added 5.3 mL (85.1 mmol) of CH_3I. After 20 min, the mixture was poured into H_2O (1000 mL) and the aqueous layer was extracted with EtOAc (3 × 1000 mL). The combined organic layers were dried (Na_2SO_4), and the solvent was evaporated. The residue was chromatographed on flash silica (600 g) with EtOAc/CH_2Cl_2 (5:95) to yield 19.8 g (91%) of ester **51** as a white solid. Mp: 173.5–174.5 °C (EtOAc/CH_2Cl_2 3:1) IR (KBr): 2980, 2870, 1688, 1270, 1160, 1110, 940, 750 cm^{-1}. ^1H NMR ($CDCl_3$) δ (ppm): 1.40 (s, 9 H), 2.99 (brt, 4 H, J = 5.3 Hz), 3.50 (brt, 4 H, J = 5.3 Hz), 3.96 (s, 3 H), 7.82 (d, 2 H, J = 7.4 Hz), 8.20 (d, 2 H, J = 7.4 Hz). Anal. ($C_{17}H_{24}N_2O_6S$) C, H, N, S.

1-(Bromomethyl)-4-[[4-(*tert*-butoxycarbonyl)-piperazinyl]sulfonyl]benzene (52). To a rapidly stirred solution of 19.7 g (51.0 mmol) of methyl ester **51** in 475 mL of THF at 0 °C under argon was added 116.7 mL (116.7 mmol) of a 1 M solution of DIBAL in hexanes over 5 min. After 30 min, 25 mL of a saturated aqueous solution of potassium sodium tartrate was added and the resulting mixture was stirred for 10 min. The mixture was then poured into 500 mL of 1:1 H_2O/saturated potassium sodium tartrate and the aqueous layer was extracted with CH_2Cl_2 (4 × 400 mL). The combined organic layers were dried (Na_2SO_4), and the solvent was evaporated. The crude residue was chromatographed on flash silica (500 g) with EtOAc/CH_2Cl_4 (1:4) to yield 17.0 g (93%) of the desired alcohol 1-(hydroxymethyl)-4-[[4-(*tert*-butoxycarbonyl)piperazinyl]-sulfonyl]benzene as a white solid. Mp: 170–171.5 °C (EtOAc/CH_2Cl_2, 1:1). IR (KBr): 3450, 2980, 1660, 1430, 1345, 1270, 1160, 930, 720 cm^{-1}. ^1H NMR ($CDCl_3$) δ (ppm): 1.39 (s, 9 H), 2.10 (t,

1 H, J = 5.1 Hz, OH), 2.95 (t, 4 H, J = 4.94 Hz), 3.49 (t, 4 H, J = 4.94 Hz), 4.80 (d, 2 H, J = 5.1 Hz), 7.53 (d, 2 H, J = 8.2 Hz), 7.72 (d, 2 H, J = 8.2 Hz). Anal. ($C_{16}H_{24}N_2O_5S$) C, H, N, S.

To a rapidly stirred solution of 4.4 g (16.8 mmol) of Ph_3P and 5.6 g (16.8 mmol) of CBr_4 in 80 mL of CH_2Cl_2 at 25 °C was added as a solid 4.0 g (11.2 mmol) of the above alcohol. After 20 min, the mixture was poured into H_2O (400 mL) and the aqueous layer was extracted with CH_2Cl_2 (2 × 400 mL). The combined organic layers were dried (Na_2SO_4), and the solvent was evaporated. The residue was chromatographed on flash silica (200 g) with Et_2O/CH_2Cl_2 (1.5:98.5) to yield 4.53 g (96%) of the desired bromide **52** as a white solid. Mp: 155–156 °C dec. IR (KBr): 2980, 2860, 1680, 1410, 1350, 1240, 1160, 930, 845, 740, 730 cm^{-1}. ^1H NMR ($CDCl_3$) δ (ppm): 1.40 (s, 9 H), 2.98 (t, 4 H, J = 4.9 Hz), 3.50 (t, 4 H, J = 4.9 Hz), 4.49 (s, 2 H, CH_2Br), 7.56 (d, 2 H, J = 8.3 Hz), 7.72 (d, 2 H, J = 8.3 Hz). Anal. ($C_{16}H_{23}N_2O_4SBr$) C, H, N, Br.

5-Methylbenz[*cd*]indol-2(1*H*)-one (45b). To a rapidly stirred solution of 1.023 mL (10.7 mmol) of ethyl chloroformate in 10 mL of acetone at −5 °C was added a solution of 1.00 g (5.37 mmol) of 5-methylnaphthoic acid and 1.50 mL (10.7 mmol) of TEA in 15 mL of acetone dropwise over 10 min. After stirring at −5 °C for 30 min, a solution of 0.696 g (10.7 mmol) of NaN_3 in 10 mL of H_2O was added dropwise to the mixture. After stirring at −5 °C for 30 min, the resulting slurry was poured into 100 mL of H_2O. The mixture was filtered to yield 934 mg (82%) of the desired product 5-methylnaphthoyl azide as a white solid. This material was used without further purification in the next step. Mp: 69–70 °C dec. ^1H NMR ($CDCl_3$) δ (ppm): 2.73 (s, 3 H), 7.40 (d, 1 H, J = 7.0 Hz), 7.50–7.57 (m, 2 H), 8.23–8.31 (m, 2 H), 8.92 (d, 1 H, J = 8.6 Hz).

To a pot of 40 mL of dry distilling chlorobenzene under argon was added dropwise a solution of 4.0 g (18.9 mmol) of 5-methylnaphthoyl azide (dried by azeotroping with benzene) in 40 mL of dry chlorobenzene. The mixture was distilled over a 1-h period to a viscous residue. The resulting isocyanate residue was diluted with 40 mL of nitrobenzene added to a tube containing 20 mL of condensed boron trichloride at −78 °C. The tube was sealed and heated at 110–115 °C with stirring for 28 h. After cooling to ambient temperature, the tube was opened and boron trichloride allowed to escape. The dark solution was poured into 100 mL of 0.5 N HCl. The tube was rinsed with EtOAc (2 × 5 mL) and THF (2 × 5 mL). The aqueous solution was extracted with EtOAc (3 × 50 mL). The combined extracts were washed with brine (20 mL) and dried (Na_2SO_4), and the solvent was evaporated. The residue was chromatographed on flash silica using THF/CH_2Cl_2 (5:95) to yield 1.75 g (51%) of amide **45b** as a yellow solid. Mp: 215–217 °C. ^1H NMR ($CDCl_3$) δ (ppm): 6.96 (d, 1 H, J = 7.03 Hz), 7.46 (m, dd, 1 H, J_1 = 7.13 Hz, J_2 = 8.55 Hz), 7.53 (d, 1 H, J = 7.06 Hz), 7.64 (d, 1 H, J = 8.5 Hz), 7.83 (brs, 1 H), 7.98 (d, 1 H, J = 7.1 Hz). IR (KBr): 3195, 1685, 1640, 1495, 765 cm^{-1}. Anal. ($C_{12}H_9NO$) C, H, N.

N^6-[4-(Phenylsulfonyl)benzyl]-6-aminobenz[*cd*]indol-2(1*H*)-one (55d). To a rapidly stirred solution of 300 mg (1.36 mmol) of amine **47a** and 0.57 mL (3.26 mmol) of DIEA in 5 mL of DMF at 75 °C was added 507 mg (1.6 mmol) of bromide **62a**. After 3 h, the mixture was poured into H_2O and the aqueous layer was extracted with EtOAc (3 × 100 mL). The combined organic layers were dried (Na_2SO_4), and the solvent was evaporated. The residue was crystallized from EtOH to give 403 mg (71%) of the desired product as an orange solid. Mp: 196–212 °C dec. IR (KBr): 1630, 1450, 1265, 1150, 1100, 725 cm^{-1}. ^1H NMR (DMSO-d_6) δ (ppm): 4.51 (brs, 2 H, NCH_2Ar), 6.05 (d, 1 H, J = 7.7 Hz), 6.63 (d, 1 H, J = 7.7 Hz), 7.15 (brs, 1 H, NHR), 7.55–7.75 (m, 6 H), 7.88–7.98 (m, 5 H), 8.47 (d, 1 H, J = 8.1 Hz), 10.35 (s, 1 H, NHC=O). HRMS: m/e calcd for $C_{24}H_{18}N_2O_2S$ 414.1038, found 414.1032.

N^6-[4-(Phenylsulfonyl)benzyl]-N^6-methyl-6-aminobenz[*cd*]Indol-2(1*H*)-one (30). To a rapidly stirred solution of 9.5 g (22.9 mmol) of amine **55d** and 6.0 mL (34.6 mmol) of DIEA in 40 mL of DMF at 95 °C was added 2.14 mL (34.4 mmol) of CH_3I. After 14 h, an additional 0.5 mL (8.0 mmol) of CH_3I was added. After an additional 5 h, the mixture was poured into H_2O (1 L) and filtered. The resulting solid was dissolved in CH_2Cl_2 (1 L) and washed with H_2O (3 × 50 mL). The organic layer was dried (Na_2SO_4) and the solvent was evaporated. The residue was chromatographed on flash silica (500 g) with a gradient of 40–50% THF/hexane to yield 2.53 g (26%) of amide **30** as an orange solid. Mp: 228–230 °C (EtOAc). IR (KBr): 1670, 1450, 1305, 1150, 725 cm^{-1}. ^1H NMR ($CDCl_3$) δ (ppm): 2.80 (s, 3 H, NCH_3), 4.39 (s, 2 H, NCH_2), 6.83 (d, 1 H, J = 7.6 Hz), 6.85 (d, 1 H, J = 7.6 Hz), 7.50–7.60 (m, 5 H), 7.68 (t, 1 H, J = 7.3 Hz), 7.75 (brs, 1 H, NH), 7.96 (t, 4 H, J = 8.5 Hz), 8.08 (d, 1 H, J = 7.0 Hz), 8.19 (d, 1 H, J = 8.3 Hz). HRMS: m/e calcd for $C_{25}H_{20}O_3N_2S$ 428.1195, found 428.1181. Anal. ($C_{25}H_{20}O_3N_2S$) C, H, N, S.

N^6-[4-(Phenylsulfonyl)benzyl]-N^6-methyl-2-(methylthio)-6-aminobenz[*cd*]indole (63). To a rapidly stirred solution of 547 mg (1.28 mmol) of amide **30** in 30 mL of toluene at 120 °C was added 568 mg (1.40 mmol) of Lawssen's reagent. After 1 h, the solvent was evaporated and the crude residue was chromatographed on flash silica gel (50 g) with Et_2O/CH_2Cl_2 (4:96) to yield 268 mg (47%) of the desired material *N*-[4-(phenylsulfonyl)benzyl]-*N*-methyl-6-aminobenz[*cd*]indol-2(1*H*)-thione as a red solid. Mp: 196–199 °C. IR (KBr): 3160, 1430, 1415, 1300, 1180, 1145, 1100, 925, 805, 725 cm^{-1}. ^1H NMR ($CDCl_3$) δ (ppm): 2.84 (s, 3 H, NCH_3), 4.47 (s, 2 H, NCH_2Ar), 6.85 (d, 1 H, J = 7.7 Hz), 6.98 (d, 1 H, J = 7.7 Hz), 7.49–7.61 (m, 5 H), 7.66 (t, 1 H, J = 7.3 Hz), 7.93–8.01 (m, 4 H), 8.19 (d, 1 H, J = 8.1 Hz), 8.25 (d, 1 H, J = 7.3 Hz), 9.32 (brs, 1 H, NHC=S). HRMS: m/e calcd for $C_{25}H_{20}N_2O_2S_2$ 444.0966, found 444.0963.

To a rapidly stirred solution of 265 mg (0.60 mmol) of the above thiolactam and 1.3 mL (1.31 mmol) of a 1 N aqueous NaOH solution in 10 mL of 1:1 EtOH/THF at 25 °C was added 41 μL (0.66 mmol) of CH_3I. After 30 min, the mixture was poured into H_2O (50 mL) and the aqueous layer was extracted with EtOAc (3 × 60 mL). The combined organic layers were dried (Na_2SO_4), and the solvent was evaporated. The crude residue was chromatographed on flash silica (30 g) with $EtOAc/CH_2Cl_2$ (1:9) to yield 259 mg (95%) of the desired material, compound **63**, as a red solid. Mp: 209–210 °C. IR (KBr): 2800, 1410, 1300, 1200, 1145, 1100, 920, 810, 770, 720 cm^{-1}. ^1H NMR ($CDCl_3$) δ (ppm): 2.84 (s, 3 H), 2.89 (s, 3 H), 4.57 (s, 2 H, NCH_2Ar), 6.84 (d, 1 H, J = 7.6 Hz), 7.48–7.62 (m, 7 H), 7.85 (d, 1 H, J = 7.0 Hz), 7.93–8.00 (m, 4 H), 8.03 (d, 1 H, J = 8.1 Hz). HRMS: m/e calcd for $C_{26}H_{22}N_2O_2S_2$ 458.1123, found 458.1107.

N^6-Methyl-N^6-[[4-(phenylsulfonyl)phenyl]methyl]-6-aminobenz[*cd*]indole-2,6-diamine (12). A mixture of 255 mg (0.56 mmol) of methyl thioether **63** in 10 mL of MeOH saturated with NH_3 was heated in a sealed tube to 145 °C for 5 h. After cooling, the solvent was evaporated and the crude residue was chromatographed on flash silica gel (30 g) with $MeOH/CH_2Cl_2$ (1:9) to yield 207 mg (87%) of amidine **12** as a red foam. IR (KBr): 2840, 1610, 1410, 1295, 1215, 1140, 1090, 1050, 805, 720 cm^{-1}. ^1H NMR (DMSO-d_6) δ (ppm): 2.83 (s, 3 H, NCH_3), 4.46 (s, 2 H, NCH_2Ar), 6.86 (d, 1 H, J = 7.6 Hz), 7.16 (d, 1 H, J = 7.6 Hz), 7.49–7.61 (m, 5 H), 7.66 (t, 1 H, J = 8.1 Hz), 7.92–8.02 (m), 8.20 (d, 1 H, J = 8.2 Hz), 8.55 (d, 1 H, J = 7.2 Hz).

***N*-Hydroxy-4-nitro-1,8-naphthalimide (57).**[23] A stirred solution of 252 g (1.04 mol) of 4-nitro-1,8-naphthalic anhydride **56**, 86.1 g (1.24 mol) of hydroxylamine hydrochloride, and 102 g (1.24 mol) of sodium acetate in 2.5 L of distilled water was heated to 80 °C. After 3 h, the mixture cooled to below 50 °C, and the product collected by filtration. The filter cake was washed with H_2O and dried at 80 °C under vacuum to yield 275.6 g of crude product (103%). TLC showed the material to be one spot. The bulk of the product was used as is in subsequent reactions. A portion (12.8 g) was recrystallized from acetic acid to yield 9.6 g (75%) of pure product. Mp: 256.5–258.5 °C (lit.[23] mp: 260–261 °C). IR (KBr): 3198, 3090, 1725, 1527, 1336, 1253, 1030, 750 cm^{-1}. ^1H NMR (DMSO-d_6/TMS) δ (ppm): 8.09 (t, 1 H, J = 7 Hz), 8.63 (m, 4 H), 11.01 (bs, 1 H). Anal. ($C_{12}H_6N_2O_5$) C, H, N.

***N*-(2,4-Dinitrophenoxy)-4-nitronaphthalimide (58).** A solution of 250 g (0.968 mol) of imide **57**, 63.0 g (0.508 mol) of $Na_2CO_3 \cdot H_2O$, and 235 g (1.16 mol) of 1-chloro-2,4-dinitrobenzene in 2500 mL of distilled water was heated to reflux. After 1 h, the reaction vessel was cooled to below 50 °C and the mixture filtered. The resultant filter cake was washed with H_2O, and the wet cake was slurried in 1 L of refluxing MeOH, then cooled in an ice bath and filtered, and the filter cake was rinsed with fresh MeOH and dried to yield 385.6 g (93.9% theory) of crude product. Mp: 276–277.5 °C (lit.[23] mp: 284–284.5 °C). IR (KBr): 3110, 1703, 1607, 1535, 1348, 1231, 957, 835 cm^{-1}. ^1H NMR (DMSO-d_6/TMS)

δ (ppm): 8.15 (m, 2 H), 8.44 (dd, 1 H, J = 2, 7 Hz), 8.58 (d, 1 H, J = 8 Hz), 8.65 (m, 2 H), 8.75 (d, 1 H, J = 8 Hz), 8.95 (d, 1 H, J = 2 Hz). Anal. ($C_{18}H_8N_4O_9$) C, H, N.

5-Nitrobenz[*cd*]indol-2(1*H*)-one (59). To a solution of 24.2 g (0.605 mol) of NaOH, 480 mL of H_2O, and 1125 mL of EtOH at 25 °C was added 64.2 g (0.151 mol) of imide **58**. After 16 h, approximately 50% of the reaction solvent was evaporated. To the remaining solution was added 800 mL of distilled H_2O. The resultant mixture was gravity filtered and the filter cake discarded. The pH of the filtrate was adjusted to 3 with 98% sulfuric acid and this mix was heated to 70 °C. Some foaming was observed. The mixture was filtered hot. The filter cake was washed with chlorobenzene. The wet filter cake was extracted with hot chlorobenzene; the chlorobenzene was cooled, filtered, and dried to yield 17.7 g (55%) of a 5:1 mixture of 5-nitro- and 6-nitrobenz[*cd*]indol-2(1*H*)-one. This material was carried directly into the subsequent reduction without further purification. IR (KBr): 3175, 1715, 1522, 1339, 1252, 780 cm^{-1}. ^{1}H NMR (major isomer) (DMSO-d_6/TMS) δ (ppm): 7.1 (d, 1 H, J = 7 Hz), 7.75 (t, 1 H, J = 4 Hz), 8.05 (d, 1 H, J = 8 Hz), 8.17 (d, 1 H, J = 7 Hz), 8.62 (d, 1 H, J = 7 Hz), 11.18 (s, 1 H).

5-Aminobenz[*cd*]indol-2(1*H*)-one (60). A suspension of 33.2 g (0.155 mol) of a 5:1 mixture of benzindole **59**, 1 L of THF, and 17 g of wet Raney nickel was hydrogenated at 40 psi of H_2 for 16 h. At this point, an additional 4 g of Raney nickel was added and hydrogenation continued. After 2 h, H_2 uptake had ceased and TLC showed complete reaction. The reaction mix was vacuum filtered through diatomaceous earth, and the filtrate evaporated. The residue was refluxed in EtOAc, cooled to 0 °C, and filtered, and the filter cake washed with fresh EtOAc. The wet cake was dried under vacuum to yield 21.8 g of a reddish-green product (76%) that was 95% 5-amine (**60**) isomer by NMR. Mp: 266–269 °C. IR (KBr): 3447, 3320, 3196, 1650, 1514, 1442, 1246, 758 cm^{-1}. ^{1}H NMR (DMSO-d_6/TMS) δ (ppm): 6.70 (d, 1 H, J = 8 Hz), 6.84 (d, 1 H, J = 7 Hz), 7.0 (s, 2 H), 7.26 (t, 1 H, J = 7 Hz), 7.64 (d, 1 H, J = 8 Hz), 7.70 (d, 1 H, J = 8 Hz), 10.20 (s, 1 H). Anal. ($C_{11}H_8N_2O$·0.1H_2O) C, H, N.

5-Chlorobenz[*cd*]indol-2(1*H*)-one (45c). To a stirred solution of 8.75 g (0.065 mol) of $CuCl_2$ and 10.8 mL (8.4 g, 0.081 mol) of 90% pure *tert*-butyl nitrite in 400 mL acetonitrile was added 10.0 g (0.0543 mol) of amine **60**. After 2 h at 25 °C, the mixture was poured into a solution of 2000 mL of H_2O and 500 mL of 1 N HCl. After stirring for 30 min, the mixture was filtered, and the filter cake rinsed thoroughly with H_2O and dried over P_2O_5 to yield 10.4 g (94%) pure chloride **45c**. Mp: 264–267 °C. IR (KBr): 3180, 1736, 1638, 1491, 1250, 1098, 762 cm^{-1}. ^{1}H NMR (DMSO-d_6/TMS) δ (ppm): 7.06 (t, 1 H, J = 4 Hz), 7.61 (d, 2 H, J = 4 Hz), 7.87 (d, 1 H, J = 8 Hz), 7.97 (d, 1 H, J = 8 Hz), 10.90 (s, 1 H). Anal. ($C_{11}H_6ClNO$) C, H, N.

5-Chloro-6-nitrobenz[*cd*]indol-2(1*H*)-one (46c). To a rapidly stirred suspension of 6.0 g (29.56 mmol) of chloride **45c** in 110 mL of concentrated H_2SO_4 at 0 °C was added dropwise 2.1 mL (33.18 mmol) of concentrated nitric acid. After 3 h at 0 °C, the reaction was poured slowly into 800 mL of ice/H_2O and the precipitate was filtered, washed with H_2O, and dried. The solid remaining was a mixture of the 8-nitro and 6-nitro isomers which were separated on flash silica eluting with a gradient of hexanes/EtOAc/THF (50:50:0 to 100% THF). The mixed fractions were rechromatographed to yield a total of 5.20 g (71%) of the slower moving 5-chloro-6-nitrobenz[*cd*]indol-2(1*H*)-one. Mp: 300–304 °C. IR (KBr): 3195, 1710, 1632, 1520, 1485, 1355 cm^{-1}. ^{1}H NMR (DMSO-d_6) δ 7.07 (d, 1 H, J = 7.7 Hz), 8.10 (m, 3 H), 11.3 (s, 1 H). Anal. ($C_{11}H_5ClN_2O_3$) C, H, Cl, N.

6-Amino-5-chlorobenz[*cd*]indol-2(1*H*)-one (47c). A stirred solution of 4.25 g (17.11 mmol) of the above nitrobenz[*cd*]indole and 7.72 g (34.22 mmol) of tin(II) chloride dihydrate in 50 mL of EtOH was heated at 60 °C for 3 h. The reaction mixture was poured into 50 mL of saturated $NaHCO_3$ solution and extracted with 2 × 75 mL of EtOAc. The combined organic layers were washed with 2 × 100 mL of 0.5 N HCl. The organic layer was discarded. The aqueous layer was made basic with 6 N NaOH and reextracted with 2 × 100 mL of EtOAc. The organic layer was dried ($MgSO_4$) and evaporated to yield 2.25 g (60%) of the desired product as a dark red solid. Mp: 305 °C dec. IR (KBr): 3450, 3340, 3180, 1695, 1625, 1470 cm^{-1}. ^{1}H NMR (DMSO-d_6) δ (ppm): 5.80 (d, 2 H, J = 7.5 Hz), 6.66 (d, 1 H, J = 7.8 Hz), 6.82 (d, 1 H, J = 7.7 Hz), 7.65 (d, 1 H, J = 7.5 Hz), 7.86 (d, 1 H, J = 7.5 Hz), 10.54 (s, 1 H). HRMS: m/e calcd for $C_{11}H_7ClN_2O$ 218.0247, found 218.0246. Anal. ($C_{11}H_7Cl_1N_2O$·0.2H_2O) C, H, Cl, N.

N^6-[4-(Morpholinosulfonyl)benzyl]-6-amino-5-chlorobenz[*cd*]indol-2(1*H*)-one (55b). To a rapidly stirred solution of 567 mg (2.72 mmol) of amine **47c** and 0.52 mL (2.98 mmol) of DIEA in 30 mL of DMF at 85 °C was added 913 mg (2.85 mmol) of bromide **62b**. After 3.5 h, an additional 90 mg (0.28 mmol) of the bromide along with 0.06 mL (0.34 mmol) of base was added. After 45 min, the reaction mixture was cooled to room temperature and poured into 50 mL of ice/H_2O. The precipitate was filtered, washed with H_2O, dried, and then washed with Et_2O and dried in vacuo to yield 1.083 g (87%) of the desired material as an orange-red solid. Mp: 232–235 °C. IR (KBr): 3460, 2860, 1670, 1450, 1350, 1165 cm^{-1}. ^{1}H NMR (DMSO-d_6) δ (ppm): 2.82 (t, 4 H, J = 4.4 Hz), 3.60 (t, 4 H, J = 4.5 Hz), 4.65 (d, 2 H, J = 4.7 Hz), 6.27 (d, 1 H, J = 8.0 Hz), 6.80 (d, 1 H, J = 7.8 Hz), 6.98 (t, 1 H, J = 5.8 Hz), 7.69 (s, 4 H), 7.74 (d, 1 H, J = 7.5 Hz), 7.92 (d, 1 H, J = 7.9 Hz), 10.58 (s, 1 H). HRMS: m/e calcd for $C_{22}H_{20}ClN_3O_4S$ 457.0865, found 457.0875.

N^6-[4-(Morpholinosulfonyl)benzyl]-N^6-methyl-6-amino-5-chlorobenz[*cd*]indol-2(1*H*)-one (18). To a rapidly stirred solution of 1.028 g (2.25 mmol) of aniline **55b** and 0.43 mL (2.47 mmol) of DIEA in 15 mL of DMF at 65 °C was added 2.1 mL (33.69 mmol) of CH_3I. After 8 h at 65 °C and 18 h at 25 °C, the reaction mixture was poured into H_2O (100 mL) and the aqueous layer was extracted with EtOAc (3 × 100 mL). The combined organic layers were washed with saturated aqueous NaCl (3 × 150 mL), dried ($MgSO_4$), and evaporated. The crude residue was chromatographed on flash silica with a gradient of 10–33% EtOAc/CH_2Cl_2 to yield 0.585 g (55%) of the desired product as a yellow solid. Mp: 263–265 °C. IR (KBr): 3200 (br), 1700, 1450, 1350, 1160 cm^{-1}. ^{1}H NMR (DMSO-d_6) δ 2.66 (s, 3 H), 2.80 (t, 4 H, J = 4.4 Hz), 3.58 (t, 4 H, J = 4.5 Hz), 4.28 and 4.50 (AB, 2 H, J = 14.8 Hz), 6.92 (d, 1 H, J = 7.6 Hz), 7.20 (d, 1 H, J = 7.7 Hz), 7.66 (s, 4 H), 7.84 (d, 1 H, J = 7.5 Hz), 7.93 (d, 1 H, J = 7.5 Hz), 10.8 (s 1 H).

5-Methyl-6-nitrobenz[*cd*]indol-2(1*H*)-one (46b). To a solution of 5.2 g (28.4 mmol) of lactam **45b** in 52 mL AcOH was added 2.34 mL (36.9 mmol) of nitric acid (69–71%) and the mixture heated to ~50 °C. After 2 h, the mixture poured into 250 mL of cold H_2O and filtered. The solid was washed with CH_2Cl_2 and dissolved in ethyl acetate and filtered. The filtrate was reduced to minimum volume and the residue washed repeatedly with Et_2O and then once with CH_2Cl_2. The remaining solid was not further purified. The combined organic washings were reduced to minimum volume, and the residue was chromatographed on silica (100 g of silica: 1 g of residue) using a gradient of 0–4% THF in CH_2Cl_2 to yield a total of 3.71 g (57.2%) of the desired material as a yellow solid. Mp: 253–254 °C. ^{1}H NMR ($CDCl_3$) δ (ppm): 2.66 (s, 3 H), 6.94 (d, 1 H, J = 7.68 Hz), 7.68 (d, 1 H, J = 7.15 Hz), 7.84 (d, 1 H, J = 7.68 Hz), 8.06 (d, 1 H, J = 7.23 Hz), 8.20 (s, br, 1 H). IR (KBr): 3190 (br), 1700, 1630, 1490, 1340 cm^{-1}. Anal. ($C_{12}H_8N_2O_3$) C, H, N.

6-Amino-5-methylbenz[*cd*]indol-2(1*H*)-one (47b). 5-Methyl-6-nitrobenz[*cd*]indol-2(1*H*)-one (1.0 g, 4.4 mmol) and a catalytic amount of Raney nickel were suspended in 100 mL of freshly distilled THF. Anhydrous hydrazine (2.76 mL, 88 mmol) was added and the mixture heated under reflux. After 1.5 h, the hot mixture was filtered through Celite to remove catalyst. The filtrate was reduced to minimum volume and the residue slurried in Et_2O and then filtered to yield 0.83 g (95% crude) of the desired material. An analytical sample was obtained by chromatography on silica gel using gradient of 10–15% THF in CH_2Cl_2. Mp: 260 °C dec. ^{1}H NMR (DMSO-d_6) δ (ppm): 2.92 (s, 3 H), 5.21 (s, 2 H), 6.62 (d, 1 H, J = 7.58 Hz), 6.72 (d, 1 H, J = 7.50 Hz), 7.38 (d, 1 H, J = 7.13 Hz), 7.78 (d, 1 H, J = 7.11 Hz), 10.35 (s, 1 H). IR (KBr): 3325, 3190, 1699, 1638, 1462 cm^{-1}. Anal. ($C_{12}H_{10}N_2O$·0.35H_2O) C, H, N.

N^6-[4-(Morpholinosulfonyl)benzyl]-6-amino-5-methylbenz[*cd*]indol-2(1*H*)-one (55e). A mixture of 12.95 g (65.3 mmol) of aniline **47b**, 27.07 g (85% pure, ~72 mmol) of bromide **62b**, and 13 mL (75 mmol) of DIEA in 150 mL of DMF was stirred at 62 °C. After 3.5 h, the reaction mixture was poured into 2.5 L of cold H_2O. The precipitate was collected by filtration. The

filter cake was washed with Et_2O then slurried in CH_2Cl_2/ether and filtered to yield 27.43 g (96%) of clean product as a yellow solid. Mp: 253–255 °C. ^1H NMR (DMSO-d_6) δ (ppm): 2.82 (t, 4 H, J = 4.51 Hz), 3.06 (s, 3 H), 3.60 (t, 4 H, J = 4.53 Hz), 4.55 (d, 2 H, J = 4.67 Hz), 6.09 (t, 1 H, J = 5.16 Hz), 6.24 (d, 1 H, J = 7.83 Hz), 6.71 (d, 1 H, J = 7.68 Hz), 7.47 (d, 1 H, J = 7.33 Hz), 7.67–7.74 (m, 4 H), 7.83 (d, 1 H, J = 7.11 Hz), 10.39 (s, 1 H). IR (KBr): 1680, 1466, 1348, 1165, 1113, 945, 741 cm^{-1}. HRMS: m/e calcd for $C_{23}H_{23}N_3O_4S$ 437.1409, found 437.1390. Anal. ($C_{23}H_{23}N_3O_4S \cdot H_2O$) C, H, N, S.

N^6-[4-(Morpholinosulfonyl)benzyl]-N^6-methyl-6-amino-5-methylbenz[*cd*]indol-2(1*H*)-one (34). Aniline **55e** (29.29 g, 69 mmol) was divided into two batches. To a solution of 15.0 g (36.3 mmol) of batch I and 7 mL (40.2 mmol) of DIEA in 150 mL of DMF was added 40 mL (642 mmol) of CH_3I. The mixture was stirred at 67 °C for 6 h. To a solution of 14.29 g (32.7 mmol) of batch II and 7 mL (40.2 mmol) of DIEA in 150 mL of DMF was added 35 mL (560 mmol) of CH_3I. The mixture was stirred at 65 °C for 6.5 h. Each mixture was poured into 2200 mL of cold H_2O, and the precipitates were collected by filtration. The solids were washed with Et_2O (500 mL) and then dried. The two batches of orange solid were combined to yield 24.54 g (79%) of the desired product which was not purified further. Mp: 266–267 °C. ^1H NMR (DMSO-d_6) δ (ppm): 2.61 (s, 3 H), 2.80 (t, 4 H, J = 4.48 Hz), 3.08 (s, 3 H), 3.58 (t, 4 H, J = 4.58 Hz), 4.23, 4.43 (AB, J = 14.05 Hz), 6.85 (d, 1 H, J = 7.54 Hz), 7.18 (d, 1 H, J = 7.58 Hz), 7.55 (d, 1 H, J = 7.36 Hz), 7.58 (d, 2 H, J = 8.46 Hz), 7.66 (d, 2 H, J = 8.35 Hz), 7.86 (d, 1 H, J = 7.16 Hz), 10.59 (s, 1 H). IR (KBr): 1690, 1640, 1454, 1348, 1165, 1113, 945, 750 cm^{-1}.

N^6-[4-(Morpholinosulfonyl)benzyl]-6-aminobenz[*cd*]indol-2(1*H*)-one (55c). To a rapidly stirred solution of 6.62 g (30 mmol) of aniline **47a** and 11.5 mL (66 mmol) of DIEA in 75 mL of DMF was added 12.15 g (82% pure, 31.23 mmol) of bromide **62b**. The mixture was stirred at 105 °C for 1.5 h then 85 °C for 1.5 h. The mixture was poured into 800 mL of ice/H_2O and the precipitate collected by filtration. The solid was rinsed with Et_2O then CH_2Cl_2. The solid was dried from benzene to yield 9.59 g (75%) of the desired material as a reddish solid. Mp: 227–229 °C. IR (KBr): 3408 (br), 2855, 1694, 1460, 1163, 945, 737 cm^{-1}. ^1H NMR (DMSO-d_6) δ (ppm): 2.81 (t, 4 H, J = 4.42 Hz), 3.60 (t, 4 H, J = 4.48 Hz), 4.57 (d, 2 H, J = 5.65 Hz), 6.10 (d, 1 H, J = 7.71 Hz), 6.67 (d, 1 H, J = 7.59 Hz), 7.18 (t, 1 H, J = 5.74 Hz), 7.62–7.75 (m, 5 H), 7.96 (d, 1 H, J = 6.99 Hz), 8.50 (d, 1 H, J = 8.21 Hz), 10.39 (s, 1 H). HRMS: m/e calcd for $C_{22}H_{21}N_3O_4S$ 423.1253, found 423.1234.

N^6-[4-(Morpholinosulfonyl)benzyl]-N^6-methyl-6-aminobenz[*cd*]indol-2(1*H*)-one (25). To a solution of 0.892 g (2.1 mmol) of aniline **55c** and 0.439 mL (2.5 mmol) of DIEA in 15 mL of DMF was added 1.31 mL (21 mmol) of CH_3I and the mixture stirred at 75 °C for 85 min. The mixture was poured into 150 mL of cold H_2O then extracted with CH_2Cl_2 (4 × 75 mL). The extracts were washed with H_2O (4 × 50 mL) and brine (50 mL), dried (Na_2SO_4), and evaporated. The crude residue was purified by chromatography on silica (100:1) using a gradient of 0–1.5% MeOH in CH_2Cl_2. Recrystallization from benzene yielded 0.539 g (59%) of the desired product as a yellow solid. Mp: 200–202 °C. ^1H NMR ($CDCl_3$) δ (ppm): 2.85 (s, 3 H), 3.02 (t, 4 H, J = 4.68 Hz), 3.76 (t, 4 H, J = 4.71 Hz), 4.45 (s, 2 H), 6.88 (d, 1 H, J = 7.59 Hz), 6.92 (d, 1 H, J = 7.62 Hz), 7.62 (d, 2 H, J = 8.31 Hz), 7.70–7.77 (m, 3 H), 8.10 (d, 1 H, J = 6.95 Hz), 8.17 (s, 1 H), 8.24 (d, 1 H, J = 8.06 Hz). IR (KBr): 3154, 2847, 1701, 1472, 1346, 1167, 1113, 941, 741 cm^{-1}.

N^6-[4-(Phenylsulfonyl)benzyl]-6-amino-5-methylbenz[*cd*]indol-2(1*H*)-one (55a). To a mixture of 0.5 g (2.5 mmol) of aniline **47b** and 0.52 mL (3.0 mmol) of DIEA in 12 mL of DMF was added 1.25 g (75% pure, 3 mmol) of bromide **62a**. The mixture was stirred at 70–75 °C overnight and then poured into 150 mL of cold H_2O. The orange precipitate was collected by filtration. The solid was rinsed with Et_2O and then suspended in CH_2Cl_2 and washed with brine. The organic layer was reduced to ~10 mL in volume then diluted with Et_2O. The solid was collected by filtration to yield 0.84 g (78%) of the desired product as an orange solid. Mp: >310 °C dec. IR (KBr): 3491, 3169 (br), 1682, 1468, 1447, 1155, 1105, 733 cm^{-1}. ^1H NMR (DMSO-d_6) δ (ppm): 3.03 (s, 3 H), 4.49 (d, 2 H, J = 4.91 Hz), 6.04 (t, 1 H, J = 5.28 Hz), 6.19 (d, 1 H, J = 7.79 Hz), 6.68 (d, 1 H, J = 7.71 Hz), 7.45 (d, 1 H, J = 7.29 Hz), 7.56–7.68 (m, 5 H), 7.82 (d, 1 H, J = 7.13 Hz), 7.89–7.94 (m, 4 H), 10.36 (s, 1 H). HRMS: m/e calcd for $C_{25}H_{20}N_2O_3S$ 428.1195, found 428.1186.

N^6-[4-(Phenylsulfonyl)benzyl]-N^6-methyl-6-amino-5-methylbenz[*cd*]indol-2(1*H*)-one (16). To a solution of 0.83 g (2 mmol) of aniline **55a** and 0.418 mL (2.4 mmol) of DIEA in 15 mL of DMF was added 1.23 mL (20 mmol) of CH_3I. The mixture was stirred at 75 °C for 2 h and then at 92 °C for 1.5 h. The mixture was poured into 150 mL of cold H_2O and extracted with EtOAc (4 × 75 mL). The extracts were washed with brine, dried over Na_2SO_4, and evaporated. The residue was chromatographed on flash silica using EtOAc/CH_2Cl_2 (1:4) to yield 0.510 g (58%) of **16** as a yellow powder. Mp: 202–204 °C. ^1H NMR ($CDCl_3$) δ (ppm): 2.63 (s, 3 H), 3.11 (s, 3 H), 4.12, 4.38 (AB, J = 13.95 Hz), 6.84 (d, 1 H, J = 7.57 Hz), 7.03 (d, 1 H, J = 7.62 Hz), 7.46 (d, 2 H, J = 8.32 Hz), 7.50–7.57 (m, 4 H), 7.83 (s, 1 H), 7.87–7.99 (m, 5 H). IR (KBr): 1698, 1456, 1308, 1155, 1105, 729 cm^{-1}.

Morpholino 4-Tolyl Sulfone (61b). To a rapidly stirred solution of 27 mL (313 mmol) of morpholine in 500 mL of CH_2Cl_2 at −10 °C was added a solution of 28.6 g (150 mmol) of *p*-toluenesulfonyl chloride in 500 mL of CH_2Cl_2. The temperature was maintained at or below 0 °C for 2 h after the addition. The mixture was washed with 0.5 N HCl (3 × 150 mL) and brine (200 mL), dried (Na_2SO_4), evaporated, and filtered to yield 35.84 g (99%) of the desired material as a white solid. Mp: 149–151 °C. IR (KBr): 3055, 2976, 2853, 1597, 1454, 1346, 1165, 1115, 941 cm^{-1}. ^1H NMR ($CDCl_3$) δ (ppm): 2.45 (s, 3 H), 2.98 (t, 4 H, J = 4.72 Hz), 3.74 (t, 4 H, J = 4.73 Hz), 7.34 (d, 2 H, J = 8.24 Hz), 7.64 (d, 2 H, J = 8.28 Hz). Anal. ($C_{11}H_{15}NO_3S$) C, H, N, S.

4-(Bromomethyl)phenyl Morpholino Sulfone (62b). To a rapidly stirred solution of 4.63 g (19 mmol) of sulfonamide **61b** in 120 mL of CCl_4 and at reflux was added 3.56 g (20 mmol) of NBS. Heating continued as the refluxing mixture was exposed to 200-W light. After about 1 h, the mixture was allowed to cool to room temperature. The mixture was filtered and the filtrate washed with 0.5 N HCl (2 × 75 mL) and H_2O (75 mL) and then dried ($MgSO_4$). After evaporation, the residue was chromatographed on flash silica (100:1) using EtOAc/hexanes (1:3) to yield 2.92 g (48%) of the desired product as a white solid. Mp: 149–150 °C. IR (KBr): 2861, 1346, 1169, 1113, 947, 733 cm^{-1}. ^1H NMR ($CDCl_3$) δ (ppm): 3.01 (t, 4 H, J = 4.64 Hz), 3.74 (t, 4 H, J = 4.66 Hz), 4.50 (s, 2 H), 7.56 (d, 2 H, J = 8.27 Hz), 7.72 (d, 2 H, J = 8.26 Hz). Anal. ($C_{11}H_{14}NO_3SBr$) C, H, N, S, Br.

N^6-[4-(Phenylsulfonyl)benzyl]-N^6-methyl-2-(hydroxylamino)-6-aminobenz[*cd*]indole (14). To a suspension of 31.3 mg (0.45 mmol) of $NH_2OH \cdot HCl$ and 78 μL (0.45 mmol) of DIEA in 8 mL of THF was added 140 mg (0.3 mmol) of methyl mercaptan **63** and the mixture heated to 55 °C. After 3 h, a solution of 93 mg (1.35 mmol) of $NH_2OH \cdot HCl$ and 0.240 mL (1.4 mmol) of DIEA in 2 mL of MeOH was added. After 1 h, the solvent was evaporated and the residue dissolved in CH_2Cl_2. The organic solution was washed with H_2O, dried (Na_2SO_4), and evaporated. The residue was dissolved in THF and the product precipitated by dilution with hexanes to yield 112 mg (84%) of the desired product as a yellow solid. Mp: >185 °C dec. IR (KBr): 3356 (br), 1659, 1634, 1474, 1447, 1306, 1154, 1074, 729 cm^{-1}. ^1H NMR (DMSO-d_6) δ (ppm): 2.65 (s, 3 H), 4.27 (s, 2 H), 6.48 (d, 1 H, J = 7.59 Hz), 6.88 (d, 1 H, J = 7.73 Hz), 7.52–7.68 (m, 7 H), 7.86 (d, 1 H, J = 8.29 Hz), 7.91–7.96 (m, 4 H), 9.74 (s, 0.5 H), 10.37 (s, 0.5 H).

N^6-[4-(Phenylsulfonyl)benzyl]-N^6-methyl-6-amino-2-hydrazinobenz[*cd*]indole (13). A solution of 142 mg (0.31 mmol) of methyl mercaptan **63** in 2 mL of methanol containing 10% hydrazine was heated at 130 °C in a sealed tube. After 2.5 h, the solvent was evaporated, the residue was taken up in CH_2Cl_2, and the product was precipitated by dilution with hexanes to yield 120 mg (87%) of the desired material as brown plates. Mp: >160 °C dec. IR (KBr): 3380, 3202 (br), 1634, 1597, 1474, 1447, 1308, 1134, 1105, 814 cm^{-1}. ^1H NMR ($CDCl_3$) δ (ppm): 2.75 (s, 3 H), 4.31 (s, 2 H), 6.62 (d, 1 H, J = 7.56 Hz), 6.86 (d, 1 H, J = 7.52 Hz), 7.49–7.59 (m, 6 H), 7.77 (d, 1 H, J = 7.12 Hz), 7.91–7.98 (m, 5 H).

N^6-[4-(Phenylsulfonyl)benzyl]-N^6,N^2-dimethyl-2,6-diaminobenz[*cd*]indole (15). To 138 mg (0.3 mmol) of methyl mercaptan **63** in 2 mL of MeOH was bubbled methylamine at

0 °C for 10 min. The reaction vessel was sealed and heated at 110–120 °C. After 3 h, the heat was removed and after cooling the product was collected by filtration. The solid was rinsed with MeOH to yield after drying 100 mg (75%) of the desired material as an orange solid: mp 221–223 °C. IR (KBr): 3424, 1626, 1560, 1447, 1306, 1244, 1152, 1105, 729 cm^{-1}. ^1H NMR (DMSO-d_6) δ (ppm): 2.71 (s, 3 H), 3.03 (d, 3 H, J = 3.78 Hz), 4.38 (s, 2 H), 6.79 (d, 1 H, J = 7.54 Hz), 6.88 (d, 1 H, J = 7.48 Hz), 7.54–7.71 (m, 6 H), 7.93–7.99 (m, 6 H), 8.15 (m, 1 H).

Acknowledgment. We would like to thank the members of the Crystallography, Computational Chemistry, and Medicinal Chemistry Groups for both their intellectual and technical assistance throughout this work. We thank Dottie Olson for her expert assistance in preparing this manuscript.

Registry No. **3**·2HCl, 138384-41-5; **3** free base, 138384-42-6; **4**, 138384-43-7; **5**, 138384-44-8; **6**, 138384-45-9; **7**, 138384-46-0; **8**, 138384-47-1; **9**·maleate, 138384-49-3; **9** free base, 138384-48-2; **10**, 138384-50-6; **11**, 138384-51-7; **12**, 138384-52-8; **13**, 138384-53-9; **14**, 138384-54-0; **15**, 138384-55-1; **16**, 138384-56-2; **17**, 138384-57-3; **18**, 138384-58-4; **19**, 138384-59-5; **20**, 138384-60-8; **21**, 138384-61-9; **22** free base, 138384-62-0; **22**·HCl, 138384-63-1; **23**, 138384-64-2; **24**, 138384-65-3; **25**, 138384-66-4; **26**, 138384-67-5; **27**, 138384-68-6; **28**, 138384-69-7; **29**·$^1/_2$AcOH, 138384-71-1; **29** free base, 138384-70-0; **30**, 138384-72-2; **31**, 138384-73-3; **32**, 138384-74-4; **33**, 138384-75-5; **34**, 138384-76-6; **35**, 138384-77-7; **36**, 138384-78-8; **37**, 138407-36-0; **38**·maleate, 138384-80-2; **38** free base, 138384-79-9; **39**, 138384-81-3; **40**, 138384-82-4; **41**·xAcOH, 138384-84-6; **41** free base, 138384-83-5; **42**·2AcOH, 138384-86-8; **42** free base, 138384-85-7; **43**, 138384-87-9; **44**·maleate, 138384-89-1; **44** free base, 138384-88-0; **45a**, 130-00-7; **45b**, 138384-90-4; **45c**, 24950-29-6; **46a**, 34599-42-3; **46b**, 138384-91-5; **46c**, 138384-92-6; **47a**, 50964-11-9; **47b**, 138384-93-7; **47c**, 138384-94-8; **48**, 138384-95-9; **49**, 138384-96-0; **50**, 10130-89-9; **51**, 138384-97-1; **52**, 138384-98-2; **52** alcohol, 138384-99-3; **52** carboxylic acid, 138385-00-9; **55a**, 138384-73-3; **55b**, 138385-01-0; **55c**, 138385-02-1; **55d**, 138384-50-6; **55e**, 138385-03-2; **56**, 6642-29-1; **57**, 28434-96-0; **58**, 65300-66-5; **59**, 65300-69-8; **60**, 74356-38-0; **61b**, 6339-26-0; **62a**, 7705-63-7; **62b**, 138385-04-3; **63**, 138385-05-4; phenyl *p*-tolyl sulfone, 640-57-3; *tert*-butyl 1-piperazinecarboxylate, 57260-71-6; 5-methylnaphthoyl azide, 138385-06-5; 5-methylnaphthoic acid, 4527-60-0; *N*-[4-(phenylsulfonyl)benzyl]-*N*-methyl-6-aminobenz[*cd*]indole-2-(1*H*)-thione, 138385-07-6; 1-chloro-2,4-dinitrobenzene, 97-00-7; thymidylate synthase, 9031-61-2.

4-Substituted 2-Alkoxytetrahydrofurans as Potent and Long-Lasting PAF Antagonists

Elena Carceller,† Manuel Merlos,‡ Marta Giral,‡ Javier Bartroli,† Julián García-Rafanell,‡ and Javier Forn*

Laboratories of Chemistry and Pharmacology, Research Center, J. Uriach & Cía.S.A., Degà Bahí 59-67, 08026 Barcelona, Spain. *Received July 9, 1991*

A series of 4-substituted 2-alkoxytetrahydrofuran derivatives featuring an acetal group were prepared and evaluated for PAF antagonist activity in the PAF-induced in vitro platelet-aggregation and in vivo hypotension tests. Compound 2-[[*N*-acetyl-*N*-[[[2-(octadecyloxy)tetrahydrofuran-4-yl]methoxy]carbonyl]amino]methyl]-1-ethylpyridinium chloride (**4e**, UR-11353) was selected for further development on the basis of its high activity and long-lasting action. The compound maintained a significant activity even 24 h after administration of a single dose of 1 mg/kg iv in the PAF-induced mortality test in mice and 10 h after administration of the same dose in the PAF-induced hypotension test in rats. Comparison with previously reported carba analogues suggests that the presence of the acetal group is the structural characteristic that confers its long-lasting activity.

Introduction

Platelet activating factor (PAF), an endogenous ether-linked phospholipid identified as 1-*O*-hexadecyl and 1-*O*-octadecyl-2-acetyl-*sn*-glyceryl-3-phosphocholine[1] has been receiving increasing attention as a potential mediator of several pathological conditions such as asthma, inflammation, anaphylactic shock, gastric ulceration, and transplant rejection.[2] Shortly after PAF's biological actions were described, a wide variety of compounds exhibiting potent PAF antagonist activity were discovered.

We have recently reported a new series of disubstituted tetrahydrofuran and dioxolane derivatives of formula **1a–e** as specific PAF antagonists (Figure 1).[3] We determined the influence of ring pattern on anti-PAF activity and studied the role of the nature of the lipophilic substituent R_1. The inhibitory effect of several of these compounds in the PAF-induced rabbit platelet aggregation test was higher than that of the structurally related compound 2-[[*N*-acetyl-*N*-[[2-methoxy-3-[(octadecylcarbamoyl)-oxy]propoxy]carbonyl]amino]methyl]-1-ethylpyridinium chloride (CV-6209, **2**).[4]

In connection with our research on the role of the central framework, we have recently described a new series of linear PAF antagonists of general formula **3** as simplified models of **1a–e** derivatives.[5] These compounds feature

† Department of Chemistry.
‡ Department of Pharmacology.

(1) (a) Demopoulos, C. A.; Pinckard, N. R.; Hanahan, D. J. Platelet-activating factor. Evidence for 1-*O*-alkyl-*sn*-glycerol-3-phosphocholine as the active component (a new class of lipid chemical mediators). *J. Biol. Chem.* **1979**, *254*, 9355–9358. (b) Benveniste, J.; Tence, M.; Varenne, P.; Bidault, J.; Boullet, C.; Polonsky, J. C. Semisynthèse et structure proposeé du facteur activant les plaquettes (P. A. F.): PAF-acether, un alkyl ether analogue de la lysophosphatidylcholine. *R. Acad. Sci. Paris* **1979**, *289*, 1037–1040.

(2) Hosford, D.; Braquet, P. Antagonists of Platelet-Activating Factor: Chemistry, Pharmacology and Clinical Applications. In *Progress in Medicinal Chemistry*; Ellis, G. P., West, G. B., Eds.; Elsevier Science Publisher: Amsterdam, 1990; Vol. 27, pp 325–380.

(3) Bartroli, J.; Carceller, E.; Merlos, M.; García-Rafanell, J.; Forn, J. 1,3 Disubstituted Tetrahydrofurans and Dioxolanes as PAF-Antagonists. *J. Med. Chem.* **1991**, *34*, 373–386.

(4) (a) Terashita, Z-i.; Imura, Y.; Takatani, M.; Tsushima, S.; Nishikawa, K. CV-6209, a Highly Potent Antagonist of Platelet Activating Factor *in Vitro* and *in Vivo*. *J. Pharmacol. Exp. Ther.* **1987**, *242*, 263–268. (b) Takatani, M.; Yoshioka, Y.; Tasaka, A.; Terashita, Z.-i.; Imura, Y.; Nishikawa, K.; Tsushima, S. Platelet Activating Factor Antagonists: Synthesis and Structure-Activity Studies of Novel PAF Analogues Modified in the Phosphorylcholine Moiety. *J. Med. Chem.* **1989**, *32*, 56–64.

0022-2623/92/1835-0676$03.00/0